Supplementary Information

Selective Endocytic Trafficking in Live Cells with Fluorescent Naphthoxazoles and their Boron Complexes

Gleiston G. Dias,[a] Bernardo L. Rodrigues,[a] Jarbas M. Resende,[a] Hállen D. R. Calado,[a] Carlos A. de Simone,[b] Valter H. C. Silva,[c] Brenno A. D. Neto,[d] Marilia O. F. Goulart,[e] Fabricia R. Ferreira,[e] Assuero S. Meira,[f] Claudia Pessoa,[f,g] José R. Correa*[d] and Eufrânio N. da Silva Júnior*[a]

[a]Institute of Exact Sciences, Department of Chemistry, Federal University of Minas Gerais, 31270-901, Belo Horizonte, MG, Brazil; [b]Institute of Physics, Department of Physics and Informatics, University of São Paulo, 13560-160, São Carlos, SP, Brazil; [c]University Unit of Exact Sciences and Technology, State University of Goiás, 75024-010, Anápolis, GO, Brazil; [d]Institute of Chemistry, University of Brasilia, 70904970, P.O.Box 4478, Brasilia, DF, Brazil; [e]Institute of Chemistry and Biotechnology, Federal University of Alagoas, 57072-970, Maceió, AL, Brazil; [f]Department of Physiology and Pharmacology, Federal University of Ceará, 60430-270, Fortaleza, CE, Brazil. [g]Fiocruz-CE, 60180-900, Fortaleza, CE, Brazil.

E-mail: eufranio@ufmg.br, correa@unb.br

Contents

Chemistry

To prepare the probes from naturally occurring naphthoquinones, lapachol was initially extracted from the heartwood of *Tabebuia* sp. (*Tecoma*) and purified by a series of recrystallizations. This compound was extracted as a bright yellow solid. Using lapachol, β-lapachone was obtained by well-documented cyclization[1] using sulfuric acid as a cyclizing agent. From this compound, the fluorescent oxazole **1** was obtained in moderate yield as a white solid. The reaction of β-lapachone with salicylaldehyde in the presence of ammonium acetate in acetic acid was accomplished using a previously described methodology.[2,3,4,5] The last step consisted in preparing the π-extended planar system by complexation with boron by the reaction of **1** with BF_3 etherate, DIPEA in dichloromethane under reflux. The highly fluorescent compound **2** was obtained in high yield as a yellow solid (Scheme S1).

Compounds **3** and **4** were obtained from the inferior homologue of lapachol. In the first step, nor-lapachol was synthesized as a crystalline orange solid by Hooker oxidation methodology[6] and it was used to prepare nor-β-lapachone (nor-β-lap). From nor-β-lap, the respective luminescent compound **3** was obtained in moderate yield and after the complexation with boron in the same conditions previously discussed, compound **4** was prepared in high yield as a yellow solid with intense luminescence (Scheme S1).

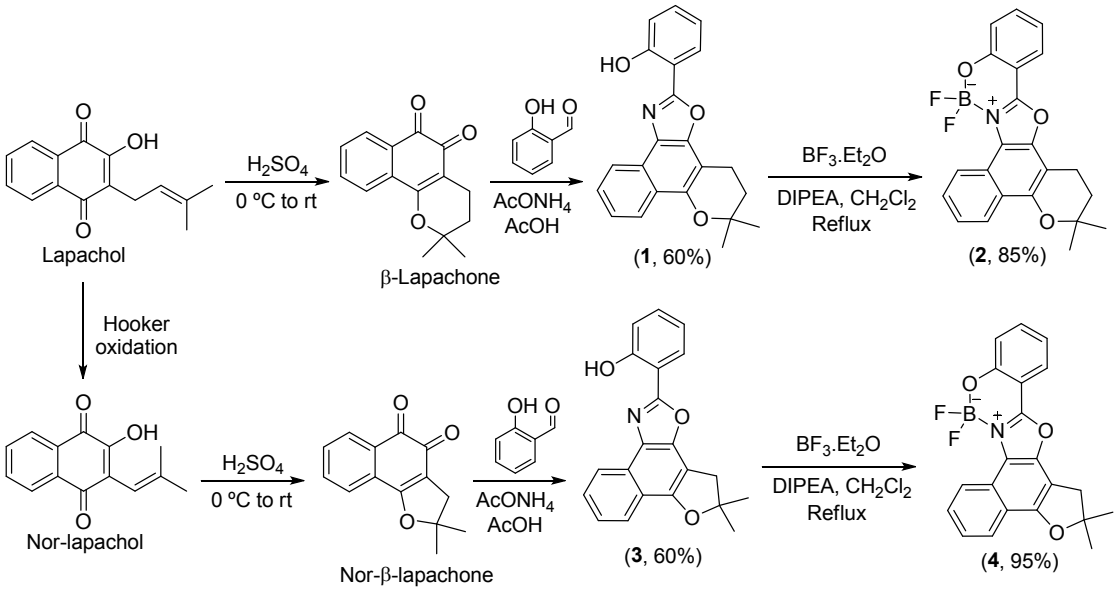

Scheme S1. Synthetic route to prepare compounds **1** and **3** and their respective boron complexes **2** and **4**.

Materials and methods

Melting points were obtained on Thomas Hoover and are uncorrected. Analytical grade solvents were used. Column chromatography was performed on silica gel (SiliaFlash G60 UltraPure 60-200 μm, 60 Å). Infrared spectra were recorded on an FTIR Spectrometer IR Prestige-21 Shimadzu. ^{1}H and ^{13}C NMR spectra were recorded at 300 K using a Bruker AVANCE DRX400 spectrometer. All samples for NMR were prepared in $CDCl_3$ containing TMS as internal reference. Chemical shifts (δ) are given in ppm and coupling constants (J) in Hertz. High resolution mass spectra (electrospray ionization) were obtained using a MicroTOF Ic – Bruker Daltonics instrument.

Synthesis of the oxazoles 1 and 3 and their boron complexes 2 and 4

Synthesis of compound 1: To a solution of β-lapachone (242 mg, 1 mmol) in acetic acid (10 mL), salicylaldehyde was added (244 mg, 0.2 mL, 2 mmol) and the mixture heated to 110 °C; ammonium acetate (1.54 g, 20 mmol) was slowly added and the reaction was monitored by thin layer chromatography, and, after eight hours, all the starting material was consumed. Then the material was brought to room temperature and added to water at 5°C. The obtained precipitate was filtered, dried and purified by column chromatography on silica gel, using as eluent a mixture of hexane/ethyl acetate. With 2% of hexane the product was eluted, and a white solid was obtained in 60 % yield (207 mg, 0.6 mmol); mp 207-208 ºC. ^{1}H NMR (400 MHz, $CDCl_3$, 300 K) δ: 1.48 (s, 6H), 1.99 (t, 2H, J = 6.7 Hz), 3.09 (t, 2H, J = 6.7 Hz), 6.99 (ddd, 1H, J = 7.8, 7.3 and 1.0 Hz), 7.12 (dd, 1H, J = 8.2 and 1.0 Hz), 7.37 (ddd, 1H, J = 8.2, 7.3 and 1.6 Hz), 7.49 (ddd, 1H, J = 8.3, 6.9 and 1.0 Hz), 7.60 (ddd, 1H, J = 8.1, 6.9 and 0.8 Hz), 8.00 (dd, 1H, J = 7.8 and 1.6 Hz), 8.28 (dd, 1H, J = 8.1 and 1.0 Hz), 8.33 (d, 1H, J = 8.3 Hz), 11.58 (s, 1H). ^{13}C NMR (100 MHz, $CDCl_3$, 300 K) δ: 17.4, 26.7, 31.6, 75.4, 101.7, 111.5, 117.2, 119.4, 121.7, 122.8, 124.1, 124.4, 124.7, 126.2, 126.9, 127.3, 132.2, 146.2, 148.1, 157.8, 160.2.

Synthesis of compound 2: In a 25 mL flask containing 10 mL of dichloromethane, the oxazole of β-lapachone (70 mg, 0.2 mmol) and 0.2 mL of $BF_3{\cdot}Et_2O$ (1.2 mmol) was added. After 5 min stirring at room temperature, 0.2 mL (1.2 mmol) of diisopropylethylamine (DIPEA) was added and the system was left under reflux. After 1 hour, the formation of a yellow precipitate was observed. The solid was filtered under

reduced pressure, and it was washed several times with dichloromethane. The product was obtained as a yellow solid without previous purification in column chromatography, and after recrystallization, it was isolated in 85% yield (66 mg, 0.8 mmol); mp 270-271 ºC. ^{1}H NMR (400 MHz, $CDCl_3$, 300 K) δ: 1.51 (s, 6H), 2.04 (t, 2H, J = 6.7 Hz), 3.16 (t, 2H, J = 6.7 Hz), 7.04 (ddd, 1H, J = 7.8, 7.3 and 0.8 Hz), 7.23 (d, 1H, J = 8.4 Hz), 7.56 (ddd, 1H, J = 8.4, 7.3 and 1.4 Hz), 7.61 (ddd, 1H, J = 8.3, 7.0 and 0.9 Hz), 7.75 (ddd, 1H, J = 8.4, 7.0 and 1.1 Hz), 7.96 (dd, 1H, J = 7.8 and 1.4 Hz), 8.37 (d, 1H, J = 8.3 Hz), 8.87 (d, 1H, J = 8.4 Hz). ^{13}C NMR (100 MHz, $CDCl_3$, 300 K) δ: 17.4, 26.7, 31.6, 75.4, 106.7, 108.3, 119.3, 119.6, 120.1, 121.4, 122.8, 123.8 (t, J = 7.0 Hz), 124.7, 124.9, 126.2, 128.6, 136.3, 147.2, 150.4, 157.8, 159.1.

Synthesis of compound 3: The same procedure to prepare compound **1** using nor-β-lapachone (228 mg, 1 mmol) in acetic acid (10 mL), salicylaldehyde (244 mg, 0.2 mL, 2 mmol) and ammonium acetate (1.54 g, 20 mmol). The product was obtained as a white solid in 60% yield (198 mg, 0.6 mmol); mp 209-210 ºC. ^{1}H NMR (400 MHz, $CDCl_3$, 300 K) δ: 1.65 (s, 6H), 3.42 (s, 2H), 6.99 (ddd, 1H, J = 7.8, 7.2, 1.1 Hz), 7.13 (ddd, 1H, J = 8.3, 1.1 and 0.3 Hz), 7.38 (ddd, 1H, J = 8.3, 7.2 and 1.6 Hz), 7.49 (ddd, 1H, J = 8.3, 6.9 and 1.2 Hz), 7.61 (ddd, 1H, J = 8.3, 6.9 and 1.2 Hz), 8.00 (ddd, 1H, J = 7.8, 1.6 and 0.3 Hz), 8.05 (ddd, 1H, J = 8.3, 1.2 and 0.8 Hz), 8.39 (ddd, 1H, J = 8.3, 1.2 and 0.8 Hz), 11.54 (s, 1H). ^{13}C NMR (100 MHz, $CDCl_3$, 300 K) δ: 20.5, 41.1, 89.1, 108.3, 122.2, 122.8, 124.8, 111.4, 117.2, 119.0, 119.5, 125.1, 126.2, 127.1, 129.2, 132.3, 144.2, 154.6, 157.6, 160.0.

Synthesis of compound 4: The same procedure to prepare compound **2** using nor-β-lapachone (45 mg, 0.2 mmol) and 0.2 mL of $BF_3{\cdot}Et_2O$ (1.2 mmol) and 0.2 mL (1.2 mmol) of diisopropylethylamine (DIPEA). The product was obtained as a yellow solid in 95% yield (72 mg, 0.9 mmol); mp 270-271ºC. ^{1}H NMR (400 MHz, $CDCl_3$, 300 K) δ: 1.69 (s, 6H), 3.49 (s, 2H), 7.08 (dd, 1H, J = 7.5 and 7.4 Hz), 7.26 (d, 1H, J = 8.2 Hz), 7.56-7.66 (m, 2H), 7.78 (dd, 1H, J = 8.6 and 7.0 Hz), 7.97 (dd, 1H, J = 7.9 and 1.3 Hz), 8.14 (d, 1H, J = 8.0 Hz), 8.94 (d, 1H, J = 8.6 Hz). ^{13}C NMR (100 MHz, $CDCl_3$, 300 K) δ: 28.4, 40.7, 90.3, 103.5, 106.7, 119.7, 119.9, 120.1, 120.4, 122.5, 122.9, 124.3 (t, J = 8.0 Hz), 124.7, 126.3, 128.9, 136.4, 145.0, 157.1, 157.8, 159.0.

NMR assignments

The unequivocal assignments of all ^{1}H and ^{13}C resonances of the oxazoles **1** and **3**, as well as of the respective boron complexes **2** and **4**, were performed by the combined analysis of the respective 1D and 2D COSY, ^{1}H-^{13}C HSQC and ^{1}H-^{13}C HMBC spectra. While multiplicity of all ^{1}H signals as well as the respective ^{1}H-^{1}H scalar coupling constants and the COSY correlations are in agreement with aromatic and aliphatic ^{1}H spin systems, the assignment of all carbon resonances was accessed by analysis of the HSQC and HMBC contour maps (see Tables S1 to S4 and Figures S2 to S28). In particular the substitution at the oxazole ring was confirmed in all cases by the HMBC correlation between the H2' resonance and most deshielded carbon resonance ($^{3}J_{H2'\text{-}C5}$ for **1** and **2** and $^{3}J_{H2'\text{-}C4}$ for **3** and **4**).

The lack of the most deshielded phenolic hydroxyl resonance on the ^{1}H NMR spectra of the boron complexes when compared to the ^{1}H NMR spectra of the respective oxazoles is an important evidence of the complexation reactions. Another important piece of information regards the downfield shift of H6 and H5 resonances on the ^{1}H NMR spectra of compounds **2** and **4**, respectively ($\Delta\delta \sim 0.6$ ppm) upon complexation, which can be attributed to the steric crowding effect imposed by the boron difluoride group. This effect seems to shield the neighboring carbons, inasmuch as significant upfield shifts are observed for **2**, C5b and C5a ($\Delta\delta$= -2.98 and -8.00 ppm, respectively) and for **4**, C4b and C4a ($\Delta\delta$ = -2.59 and -8.71 ppm, respectively). Despite this information, the most important evidences of the complexation reactions are the splittings of C6 and C5 signals in the ^{13}C NMR spectra of the complexes **2** and **4**, respectively (Figure S1). In both cases the signals appear as triplets due to the coupling with the two fluorine nuclei ($^{5}J_{F\text{-}C6}$ = 7.8 Hz for **2** and $^{5}J_{F\text{-}C5}$ = 8.0 Hz for **4**). These long range couplings are described as through space scalar spin-spin coupling constants (TSSSSCC), and several examples reported in the literature describe this sort of interaction in cases where the spin information is transmitted mainly through direct orbital interactions.[7,8] In the current case, it is more likely that overlapping between the fluorine lone pair orbitals and the C6–H6/C5–H5 antibonding orbital (LP (F)$\rightarrow\sigma^{*}$C–H) allows for the transmission of the Fermi Contact term.[9] These results unequivocally confirm the coordination of the phenol oxygen and the oxazole nitrogen to the boron atom.

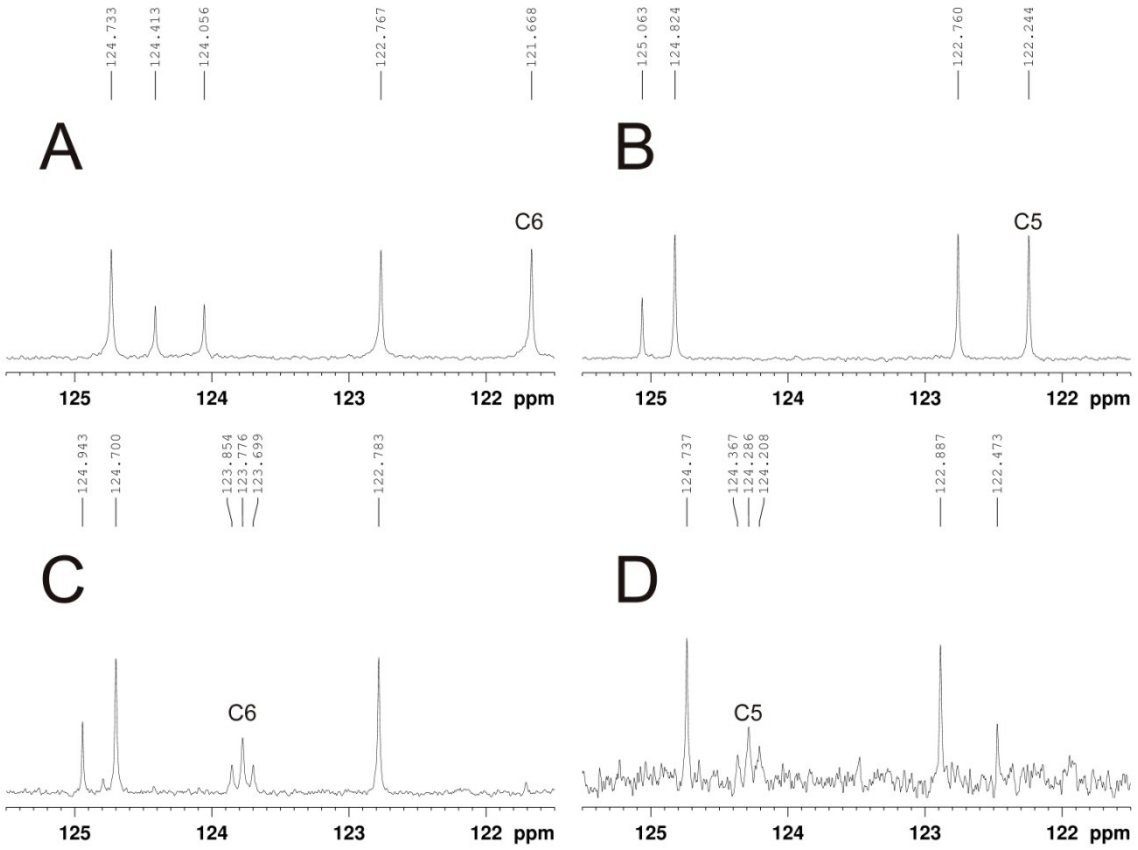

Figure S1. Expanded ^{13}C NMR spectra of (A) **1**, (B) **3**, (C) **2** and (D) **4** at 100 MHz in $CDCl_3$ (300 K).

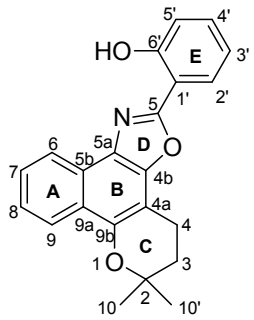

Table S1. ^{1}H and ^{13}C NMR data of **1** in $CDCl_3$ at 300 K

(^{1}H and ^{13}C data recorded at 400 and 100 MHz, respectively)

Index	δ ^{13}C/ppm	δ ^{1}H (m)/ppm [a]	^{n}J/Hz [b]	COSY (n)[b,c]	HMBC (n)[b,c]
2	75.4	-	-	-	3(2), 10/10'(2), 4(3)
3	31.6	1.99 (t)	$^{3}J_{H3\text{-}H4}$ 6.7	4(3)	4(2), 10/10'(3)
4	17.4	3.09 (t)	$^{3}J_{H3\text{-}H4}$ 6.7	3(3)	3(2), 10/10'(4)
5	160.2	-	-	-	2'(3), 5'(4,w)
6	121.7	8.28 (dd)	$^{3}J_{H6\text{-}H7}$ 8.1, $^{4}J_{H6\text{-}H8}$ 1.0	7(3), 8(4,w)	8(3)
7	126.9	7.60 (ddd)	$^{3}J_{H6\text{-}H7}$ 8.1, $^{3}J_{H7\text{-}H8}$ 6.9, $^{4}J_{H7\text{-}H9}$ 0.8	6(3), 8(3), 9(4,w)	9(3)
8	124.7	7.49 (ddd)	$^{3}J_{H7\text{-}H8}$ 6.9, $^{3}J_{H8\text{-}H9}$ 8.3, $^{4}J_{H6\text{-}H8}$ 1.0	7(3), 9(3), 6(4,w)	6(3)
9	122.8	8.33 (d)	$^{3}J_{H8\text{-}H9}$ 8.3	8(3), 7(4,w)	8(2,w), 7(3)
10/10'	26.7	1.48 (s)	-	-	3(3), 10'/10(3)
4a	101.7	-	-	-	4(2), 3(3)
4b	146.3	-	-	-	4(3)
5a	127.3	-	-	-	6(3)
5b	124.4	-	-	-	7(3), 9(3)
9a	124.1	-	-	-	6(3), 8(3), 4(4,w)
9b	148.1	-	-	-	4(3), 9(3), 6(4,w)
1'	111.5	-	-	-	3'(3), 5'(3), HO(3), 4'(4,w)
2'	126.2	8.00 (dd)	$^{3}J_{H2'\text{-}H3'}$ 7.8, $^{4}J_{H2'\text{-}H4'}$ 1.6	3'(3), 4'(4)	3'(2), 4'(3)
3'	119.4	6.99 (ddd)	$^{3}J_{H2'\text{-}H3'}$ 7.8, $^{3}J_{H3'\text{-}H4'}$ 7.3, $^{4}J_{H3'\text{-}H5'}$ 1.0	2'(3), 4'(3), 5'(4,w)	5'(3)
4'	132.2	7.37 (ddd)	$^{3}J_{H3'\text{-}H4'}$ 7.3, $^{3}J_{H4'\text{-}H5'}$ 8.2, $^{4}J_{H2'\text{-}H4'}$ 1.6	3'(3), 5'(3), 2'(4)	3'(2,w), 5'(2), 2'(3)
5'	117.2	7.12 (dd)	$^{3}J_{H4'\text{-}H5'}$ 8.2, $^{4}J_{H3'\text{-}H5'}$ 1.0	4'(3), 3'(4,w)	OH(3), 2'(4)
6'	157.8	-	-	-	OH(2), 2'(3), 4'(3)
OH	-	11.58 (s)	-	-	-

a – m = multiplicity; *b* – n = number of chemical bonds; *c* – "w" means week intensity correlation

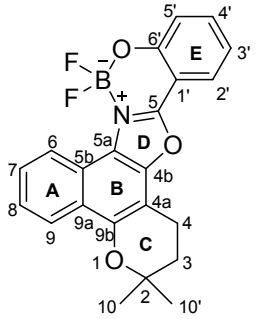

Table S2. ^{1}H and ^{13}C NMR data of **2** in $CDCl_3$ at 300 K

(^{1}H and ^{13}C data recorded at 400 and 100 MHz, respectively)

Index	δ ^{13}C/ppm	δ ^{1}H (m)/ppm [a]	^{n}J/Hz [b]	COSY (n)[b,c]	HMBC (n)[b,c]
2	75.4	-	-	-	3(2), 10/10'(2), 4(3)
3	31.6	2.04 (t)	$^{3}J_{H3\text{-}H4}$ 6.7	4(3)	4(2), 10/10'(3)
4	17.4	3.16 (t)	$^{3}J_{H3\text{-}H4}$ 6.7	3(3)	3(2), 10/10'(4)
5	159.1	-	-	-	2'(3), 3'(4,w), 5'(4,w), 4'(5)
6[d]	123.8	8.87 (d)	$^{3}J_{H6\text{-}H7}$ 8.4, $^{5}J_{C6\text{-}F}$ 7.0	7(3), 8(4,w)	8(3)
7	128.6	7.75 (ddd)	$^{3}J_{H6\text{-}H7}$ 8.4, $^{3}J_{H7\text{-}H8}$7.0, $^{4}J_{H7\text{-}H9}$ 1.1	8(3), 9(4,w)	9(3)
8	126.2	7.61 (ddd)	$^{3}J_{H7\text{-}H8}$ 7.0, $^{3}J_{H8\text{-}H9}$ 8.3, $^{4}J_{H6\text{-}H8}$ 0.9	9(3), 6(4,w)	6(3)
9	122.8	8.37 (d)	$^{3}J_{H8\text{-}H9}$ 8.3	8(3), 7(4,w)	8(2,w), 7(3)
10/10'	26.7	1.51 (s)	-	-	3(3), 10'/10(3)
4a	108.3	-	-	-	4(2), 3(3)
4b	147.2	-	-	-	4(3)
5a	119.2	-	-	-	6(3), 4(4,w)
5b	121.4	-	-	-	6(2,w), 7(3), 9(3)
9a	124.9	-	-	-	6(3), 8(3), 4(4,w)
9b	150.4	-	-	-	4(3), 9(3), 6(4,w)
1'	106.7	-	-	-	3'(3), 5'(3), 4'(4,w)
2'	124.7	7.96 (dd)	$^{3}J_{H2'\text{-}H3'}$ 7.8, $^{4}J_{H2'\text{-}H4'}$ 1.4	3'(3), 4'(4)	3'(2,w), 4'(3)
3'	120.1	7.04 (ddd)	$^{3}J_{H2'\text{-}H3'}$ 7.8, $^{3}J_{H3'\text{-}H4'}$ 7.3, $^{4}J_{H3'\text{-}H5'}$ 0.8	2'(3), 4'(3)	5'(3)
4'	136.3	7.56 (ddd)	$^{3}J_{H3'\text{-}H4'}$ 7.3, $^{3}J_{H4'\text{-}H5'}$ 8.4, $^{4}J_{H2'\text{-}H4'}$ 1.4	3'(3), 5'(3), 2'(4)	3'(2,w), 2'(3)
5'	119.6	7.23 (d)	$^{3}J_{H4'\text{-}H5'}$ 8.4	4'(3)	3'(3), 2'(4,w),
6'	157.8	-	-	-	5'(2,w), 2'(3), 4'(3), 3'(4,w),

a – m = multiplicity; *b* – n = number of chemical bonds; *c* – "w" means week intensity correlation; *d* – C6 signal appears as a triplet due to coupling with two fluorine atoms

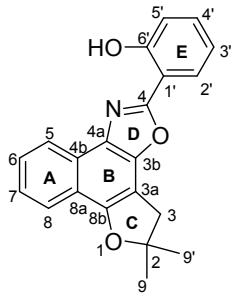

Table S3. ^{1}H and ^{13}C NMR data of **3** in $CDCl_3$ at 300 K

(^{1}H and ^{13}C data recorded at 400 and 100 MHz, respectively)

Index	δ ^{13}C/ppm	δ ^{1}H(m)/ppm [a]	^{n}J/Hz [b]	COSY (n) [b,c]	HMBC (n) [b,c]
2	89.1	-	-	-	3(2), 9/9'(2)
3	41.1	3.42 (s)	-	-	9/9'(3)
4	160.0	-	-	-	2'(3), 5'(4,w)
5	122.2	8.39 (ddd)	$^{3}J_{H5\text{-}H6}$ 8.3, $^{4}J_{H5\text{-}H7}$ 1.2, $^{5}J_{H5\text{-}H8}$ 0.8	6(3), 7(4,w)	7(3), 3(6,w)
6	127.1	7.61 (ddd)	$^{3}J_{H5\text{-}H6}$ 8.3, $^{3}J_{H6\text{-}H7}$ 6.9, $^{4}J_{H6\text{-}H8}$ 1.2	5(3), 7(3), 8(4,w)	7(2,w), 8(3)
7	124.8	7.49 (ddd)	$^{3}J_{H6\text{-}H7}$ 6.9, $^{3}J_{H7\text{-}H8}$ 8.3, $^{4}J_{H5\text{-}H7}$ 1.2	6(3), 8(3), 5(4,w)	5(3)
8	122.8	8.05 (ddd)	$^{3}J_{H7\text{-}H8}$ 8.3; $^{4}J_{H6\text{-}H8}$ 1.2; $^{5}J_{H5\text{-}H8}$ 0.8	7(3), 6(4,w)	7(2,w), 6(3), 5(4,w), 3(5,w)
9/9'	20.5	1.65 (s)	-	-	3(3), 9'/9(3)
3a	108.3	-	-	-	3(2)
3b	144.2	-	-	-	3(3)
4a	129.2	-	-	-	5(3), 3(4,w), 8(4,w)
4b	125.1	-	-	-	6(3), 8(3), 7(4,w), 3(5,w)
8a	119.0	-	-	-	5(3), 7(3), 3(4,w)
8b	154.6	-	-	-	3(3), 8(3), 5(4,w)
1'	111.4	-	-	-	3'(3), 5'(3), 4'(4,w)
2'	126.2	8.00 (ddd)	$^{3}J_{H2'\text{-}H3'}$ 7.8, $^{4}J_{H2'\text{-}H4'}$ 1.6, $^{5}J_{H2'\text{-}H5'}$ 0.3	3'(3), 4'(4)	3'(2,w), 4'(3)
3'	119.5	6.99 (ddd)	$^{3}J_{H2'\text{-}H3'}$ 7.8, $^{3}J_{H3'\text{-}H4'}$ 7.2, $^{4}J_{H3'\text{-}H5'}$ 1.1	2'(3), 4'(3), 5'(4,w)	5'(3)
4'	132.3	7.38 (ddd)	$^{3}J_{H3'\text{-}H4'}$ 7.2, $^{3}J_{H4'\text{-}H5'}$ 8.3, $^{4}J_{H2'\text{-}H4'}$ 1.6	3'(3), 5'(3), 2'(4)	3'(2,w), 2'(3)
5'	117.2	7.13 (ddd)	$^{3}J_{H4'\text{-}H5'}$ 8.3, $^{4}J_{H3'\text{-}H5'}$ 1.1, $^{5}J_{H2'\text{-}H5'}$ 0.3	4'(3), 3'(4)	4'(2,w), 3'(3), 2'(4,w),
6'	157.6	-	-	-	5'(2,w), 2'(3), 4'(3), 3'(4,w),
OH	-	11.54 (s)	-	-	-

a – m = multiplicity; *b* – n = number of chemical bonds; *c* – "w" means week intensity correlation

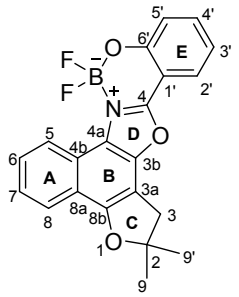

Table S4. ^{1}H and ^{13}C NMR data of **4** in $CDCl_3$ at 300 K

(^{1}H and ^{13}C data recorded at 400 and 100 MHz, respectively)

Index	δ ^{13}C/ppm	δ ^{1}H (m)/ppm [a]	^{n}J/Hz [b]	COSY (n)[b,c]	HMBC (n)[b,c]
2	90.3	-	-	-	3(2), 9/9'(2)
3	40.7	3.45 (s)	-	-	9/9'(3)
4 [d]	159.0	-	-	-	2'(3)
5[e]	124.3	8.94 (d)	$^{3}J_{H5\text{-}H6}$ 8.6, $^{5}J_{C5\text{-}F}$ 8.0	6(3), 7(4,w)	7(3)
6	128.9	7.78 (dd)	$^{3}J_{H5\text{-}H6}$ 8.6,$^{3}J_{H6\text{-}H7}$ 7.0	5(3), 7(3), 8(4,w)	8(3)
7	126.3	7.56-7.66 (m)	-	6(3), 8(3), 5(4)	5(3)
8	122.9	8.14 (d)	$^{3}J_{H7\text{-}H8}$ 8.0	7(3), 6(4,w)	6(3)
9/9'	28.4	1.69	-	-	3(3), 9'/9(3)
3a	103.5	-	-	-	3(2)
3b[d]	145.0	-	-	-	3(3)
4a[d]	120.4	-	-	-	5(3), 3(4,w)
4b	122.5	-	-	-	6(3), 8(3)
8a	119.9	-	-	-	5(3), 7(3), 3(4,w)
8b	157.1	-	-	-	3(3), 8(3)
1'	106.7	-	-	-	3'(3), 5'(3)
2'	124.7	7.97 (dd)	$^{3}J_{H2'\text{-}H3'}$ 7.9,$^{4}J_{H2'\text{-}H4'}$ 1.3	3'(3), 4'(4)	4'(3)
3'	120.1	7.08 (dd)	$^{3}J_{H2'\text{-}H3'}$ 7.4,$^{3}J_{H3'\text{-}H4'}$ 7.5	2'(3), 4'(3), 5'(4,w)	5'(3)
4'	136.4	7.56-7.66 (m)	-	3'(3), 5'(3), 2'(4,w)	2'(3)
5'	119.7	7.26 (d)	$^{3}J_{H4'\text{-}H5'}$ 8.2	4'(3), 3'(4)	3'(3)
6' [d]	157.8	-	-	-	2'(3), 4'(3)

a – m = multiplicity; *b* – n = number of chemical bonds; *c* – "w" means week intensity correlation; *d* – C4, C3b, C4a and C6' resonances were accessed only through inverse detection – Figures S24 to S27; *e* – C5 signal appears as a triplet due to coupling with two fluorine atoms

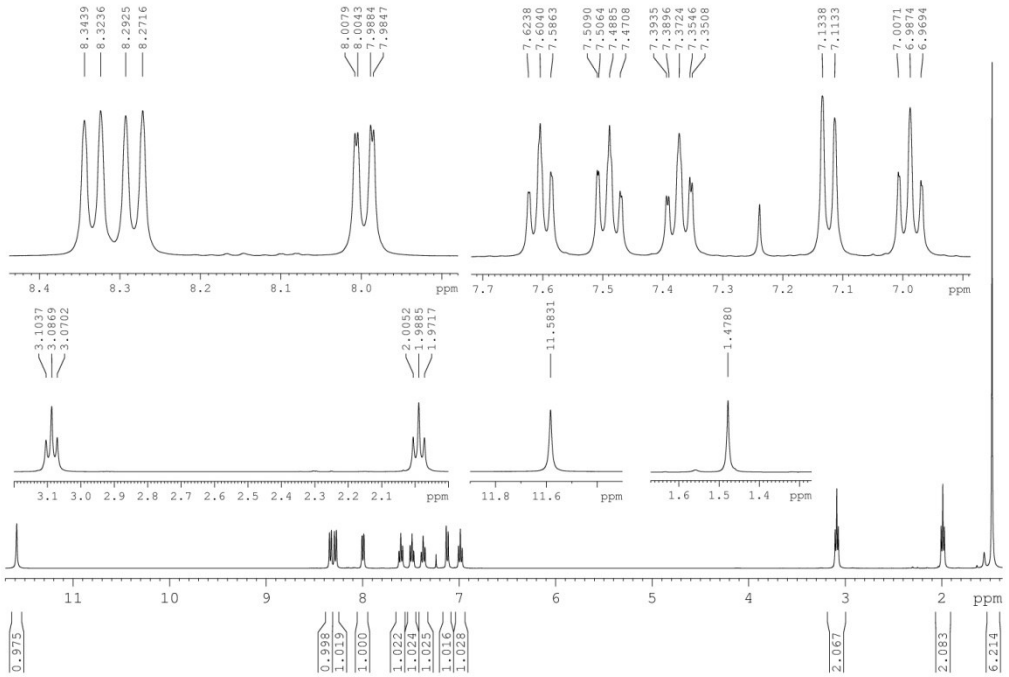

Figure S2. [1]HNMR spectrum of **1** at 400 MHz in $CDCl_3$ (300 K).

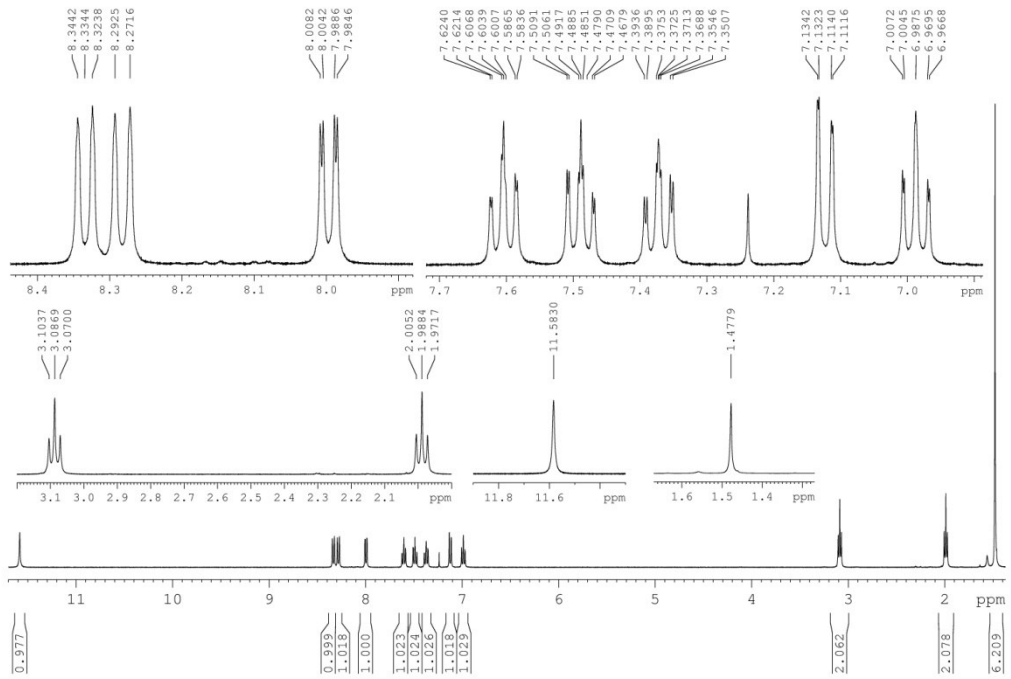

Figure S3. [1]H NMR spectrum of **1** at 400 MHz in $CDCl_3$ (300 K). Lorentz-Gauss transformation (lb = -0.5, gb =50 %).

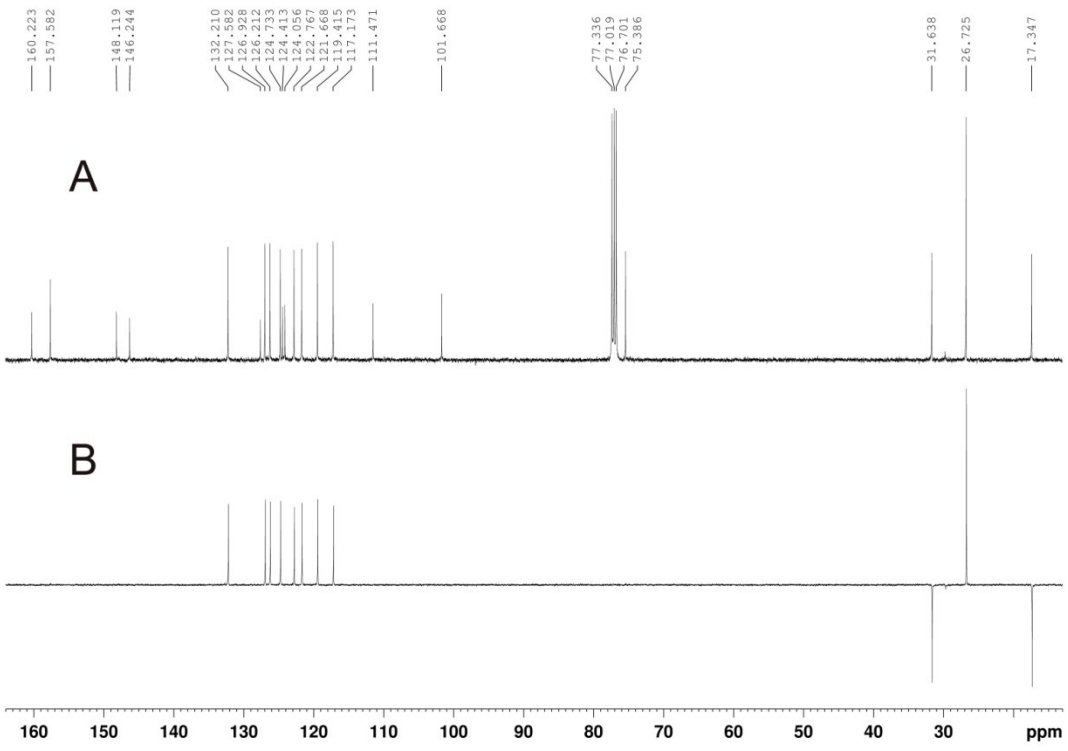

Figure S4. (A) ^{13}C NMR and (B) DEPT-135 spectra of **1** at 100 MHz in $CDCl_3$ (300 K).

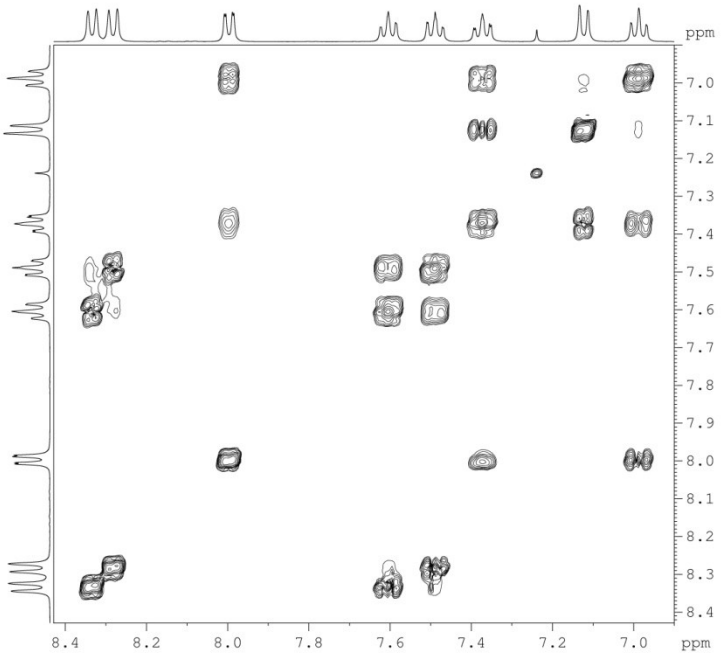

Figure S5. Expanded COSY spectrum of **1** at 400 MHz in $CDCl_3$ (300 K) showing the correlations between aromatic ^1H resonances.

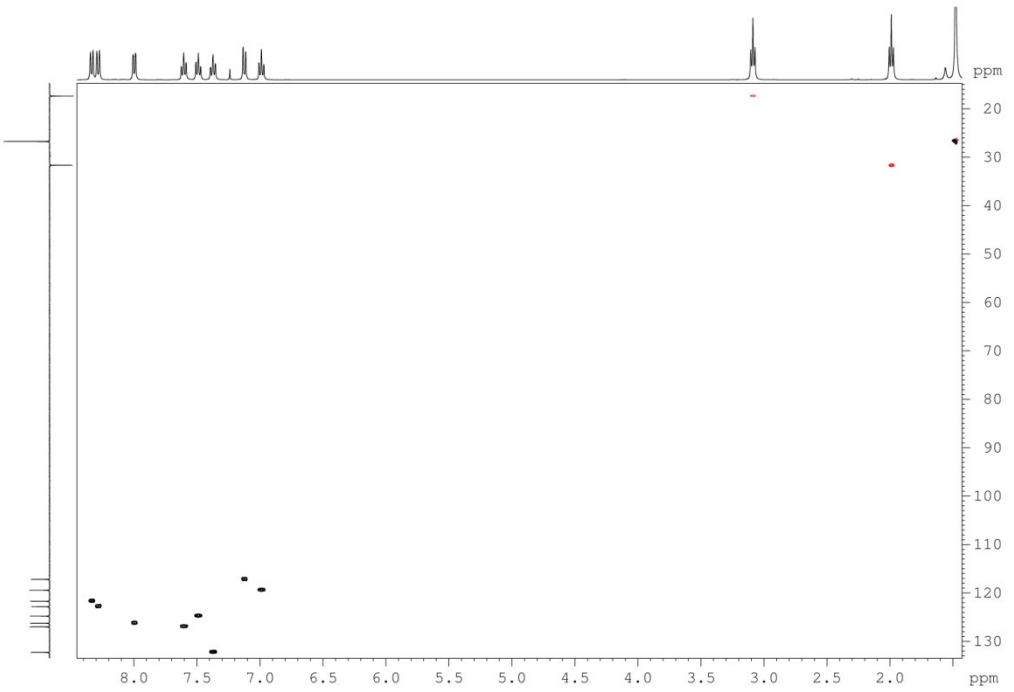

Figure S6. ^{1}H-^{13}C HSQC spectrum of **1** at 400 MHz in $CDCl_3$ (300 K). Correlations in black represent peaks with positive phase (CH_3 and CH correlations) whereas correlations in red indicate negative intensities (CH_2 correlations).

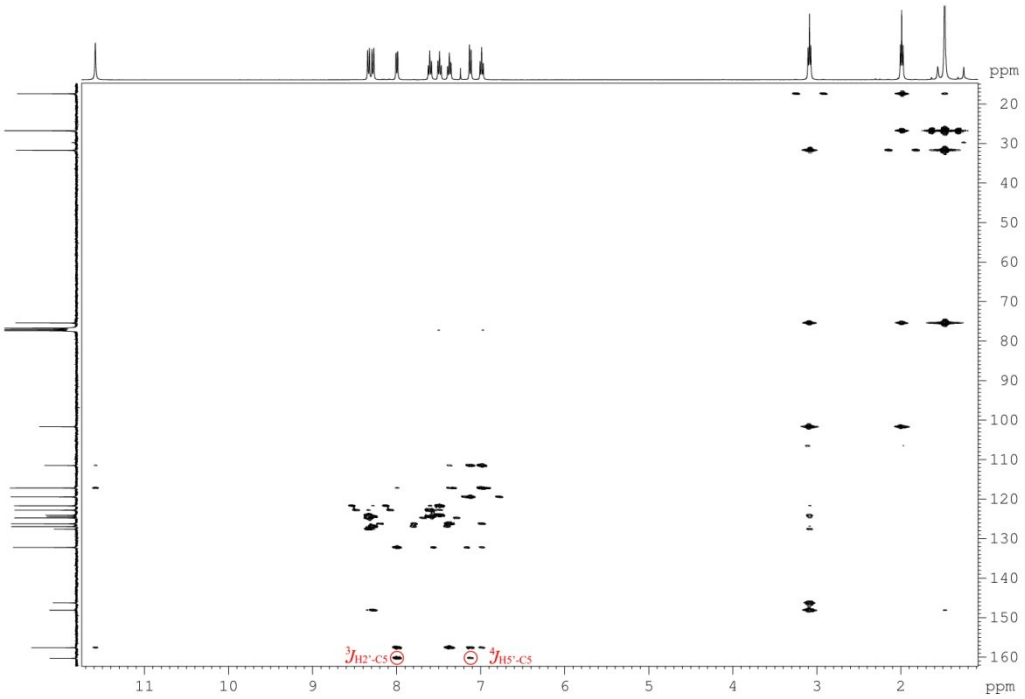

Figure S7. ^{1}H-^{13}C HMBC spectrum of **1** at 400 MHz in $CDCl_3$ (300 K).

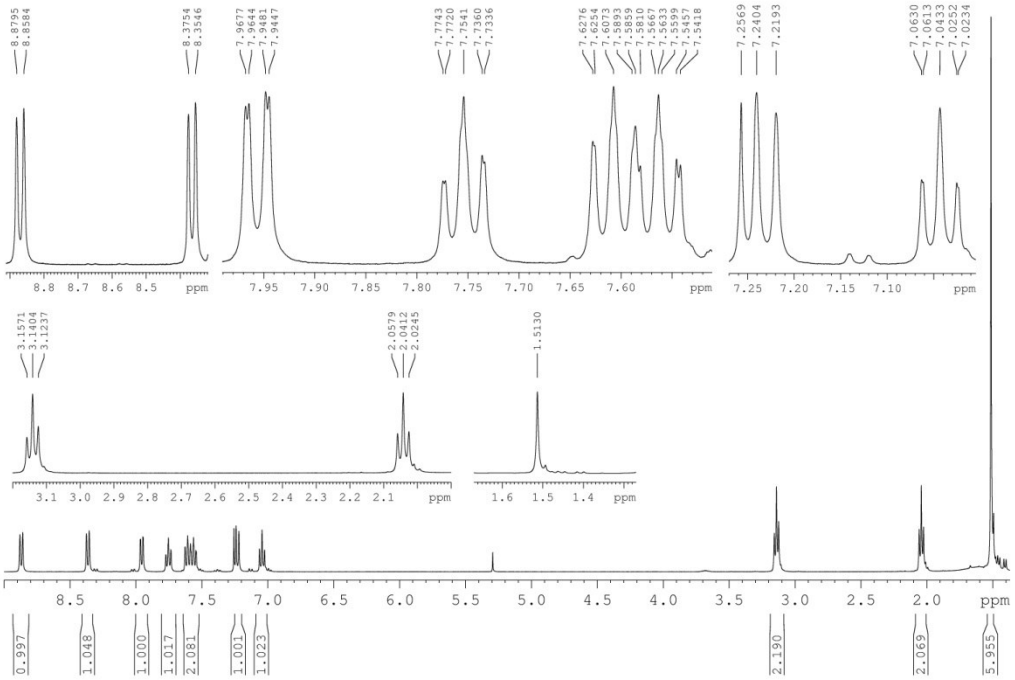

Figure S8. ^{1}H NMR spectrum of **2** at 400 MHz in $CDCl_3$ (300 K).

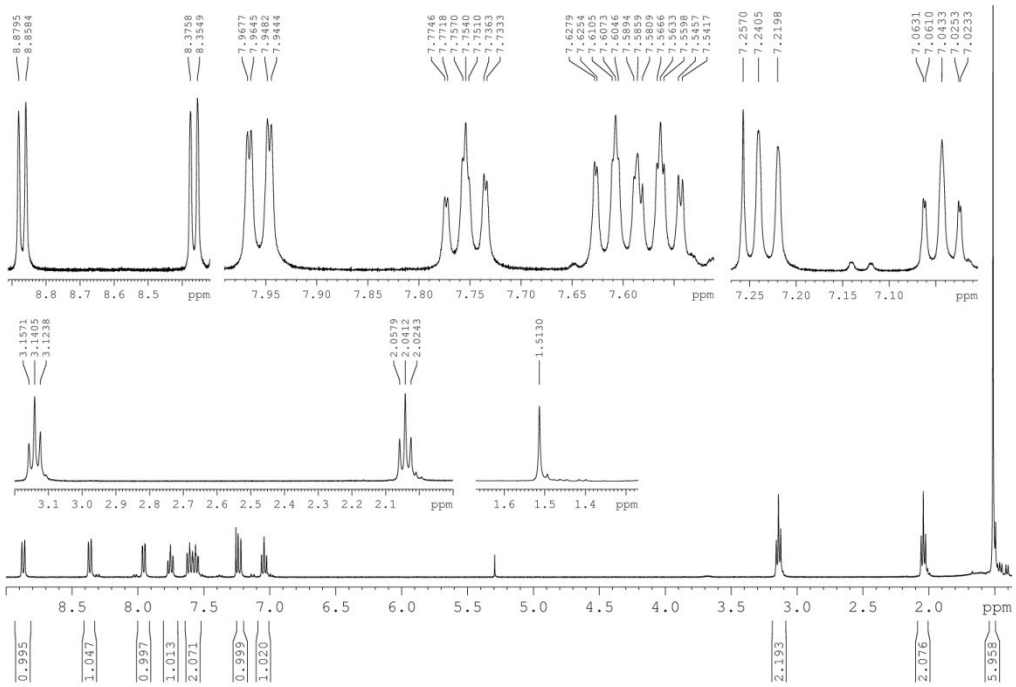

Figure S9. ^{1}H NMR spectrum of **2** at 400 MHz in $CDCl_3$ (300 K). Lorentz-Gauss transformation (lb = -0.3, gb = 40 %).

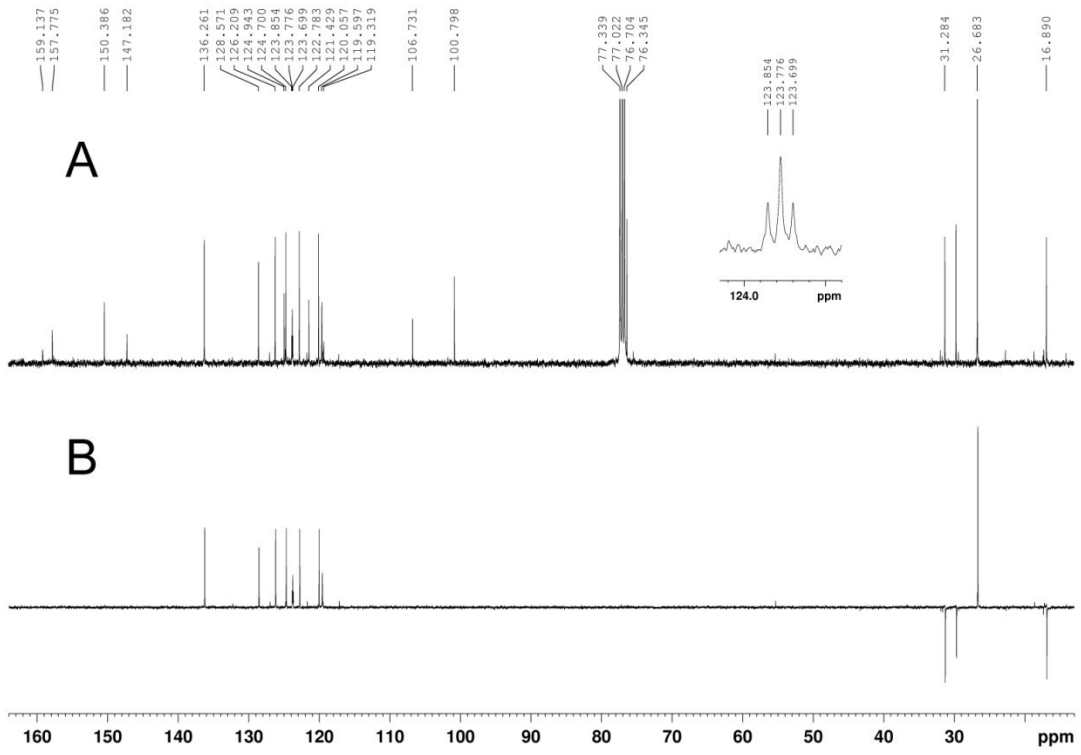

Figure S10. (A) ^{13}C NMR and (B) DEPT-135 spectra of **2** at 100 MHz in $CDCl_3$ (300 K).

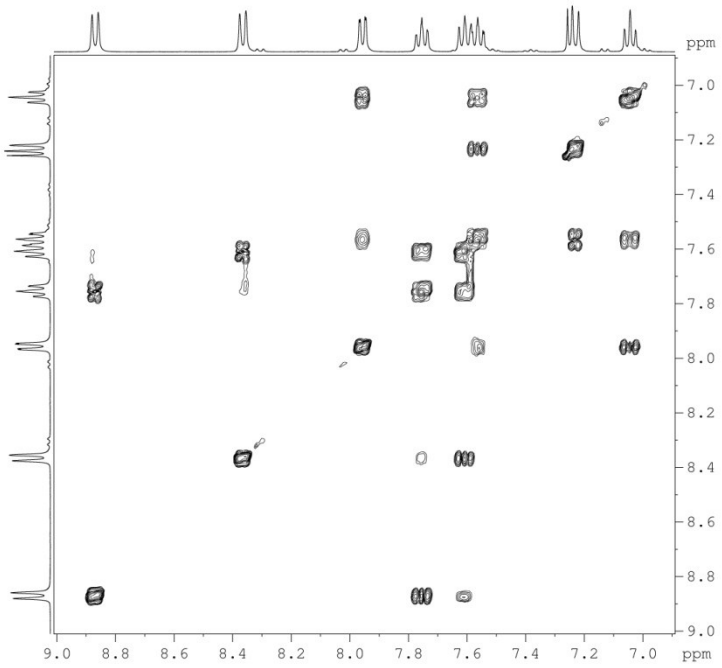

Figure S11. Expanded COSY spectrum of **2** at 400 MHz in $CDCl_3$ (300 K) showing the correlations between aromatic ^1H resonances.

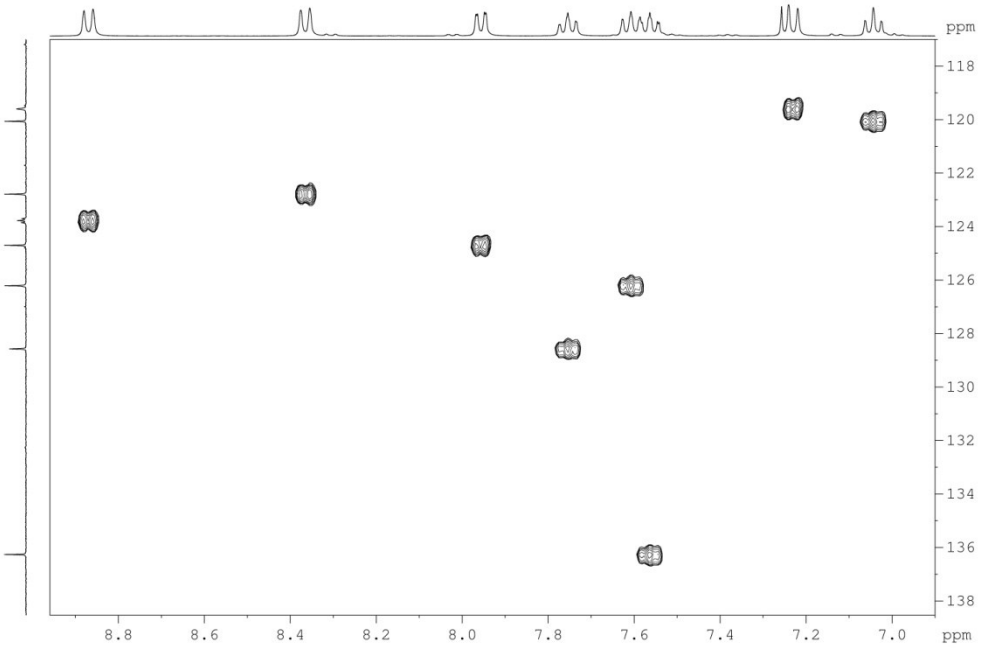

Figure S12. Expanded ^{1}H-^{13}C HSQC spectrum of **2** at 400 MHz in $CDCl_3$ (300 K) showing the correlations between aromatic ^{1}H and ^{13}C resonances.

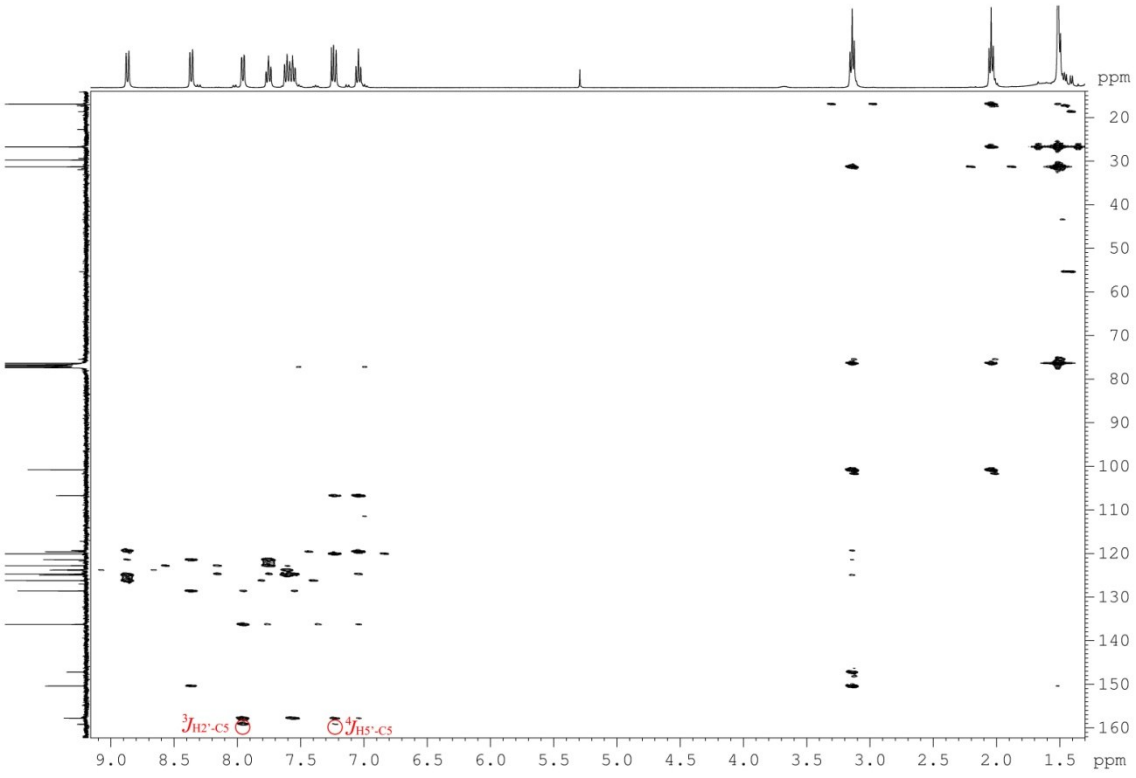

Figure S13. ^{1}H-^{13}C HMBC spectrum of **2** at 400 MHz in $CDCl_3$ (300 K).

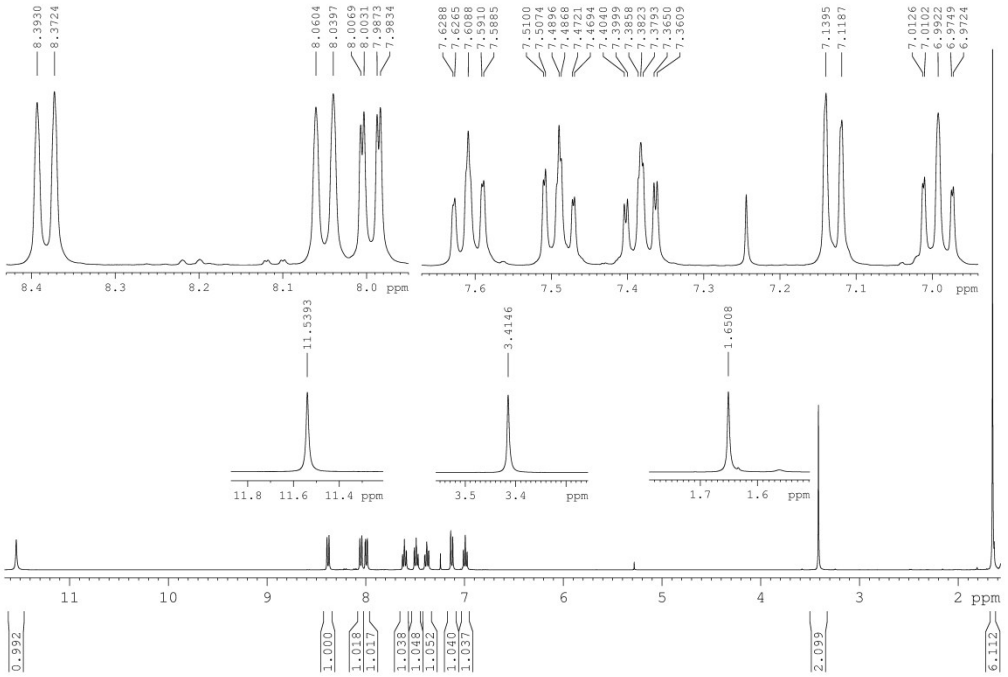

Figure S14. ^{1}H NMR spectrum of **3** at 400 MHz in $CDCl_3$ (300 K).

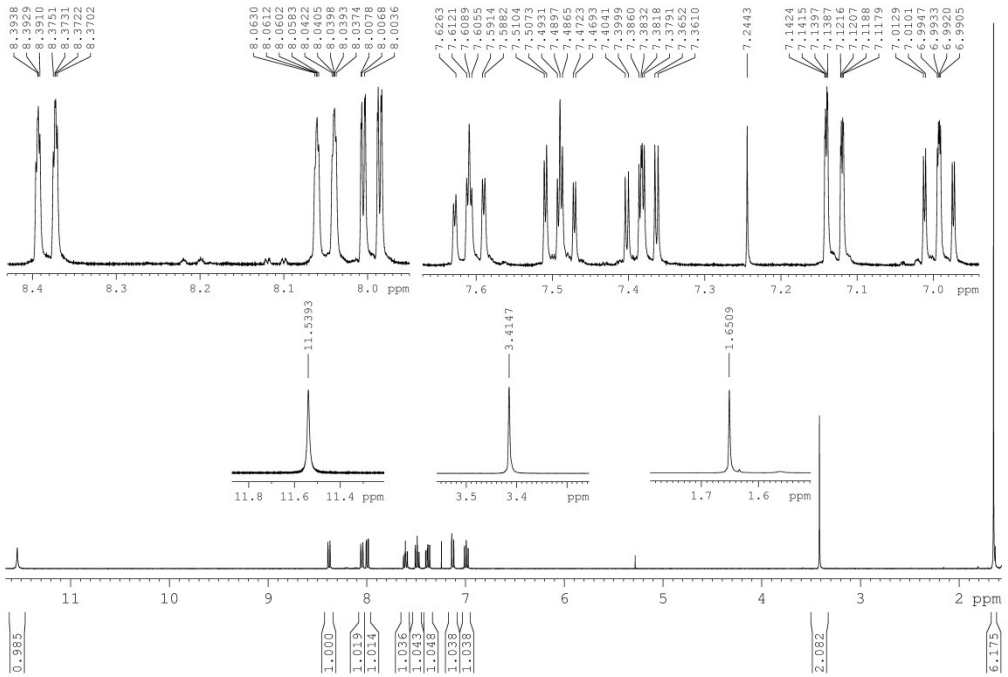

Figure S15. ^{1}H NMR spectrum of **3** at 400 MHz in $CDCl_3$ (300 K). Lorentz-Gauss transformation (lb = -0.5, gb = 50 %).

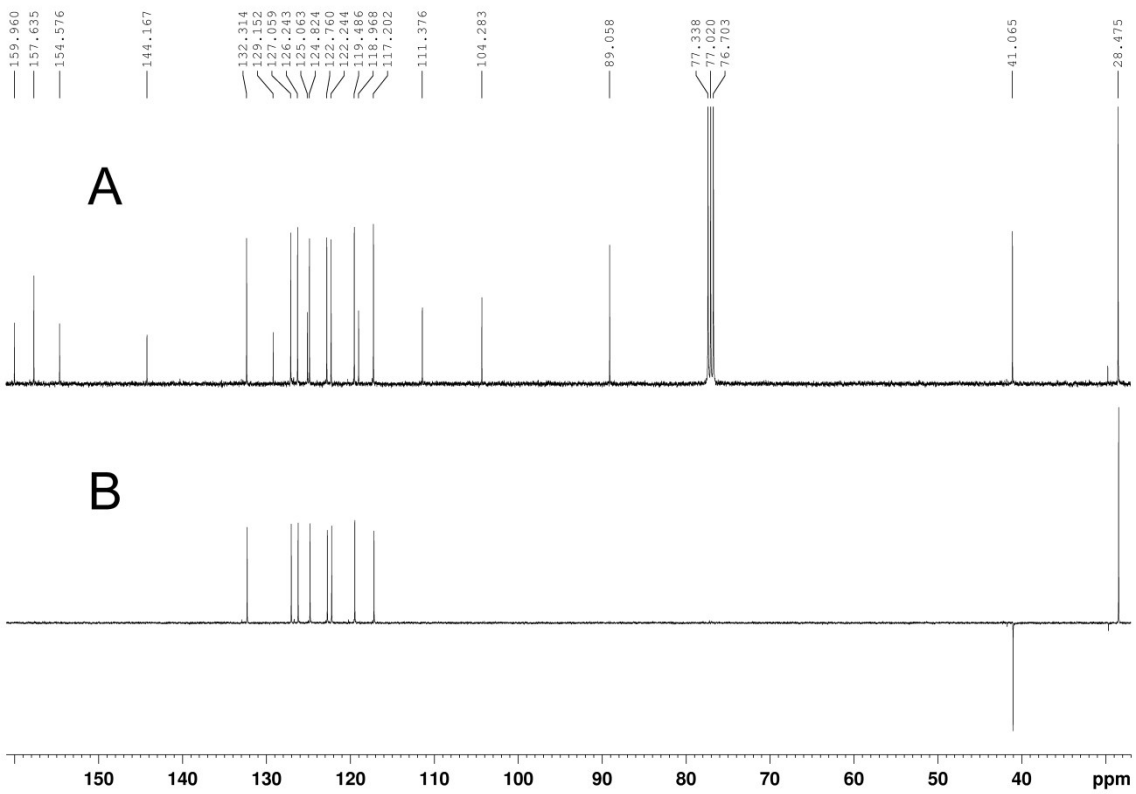

Figure S16. (A) ^{13}C NMR and (B) DEPT-135 spectra of **3** at 100 MHz in $CDCl_3$ (300 K).

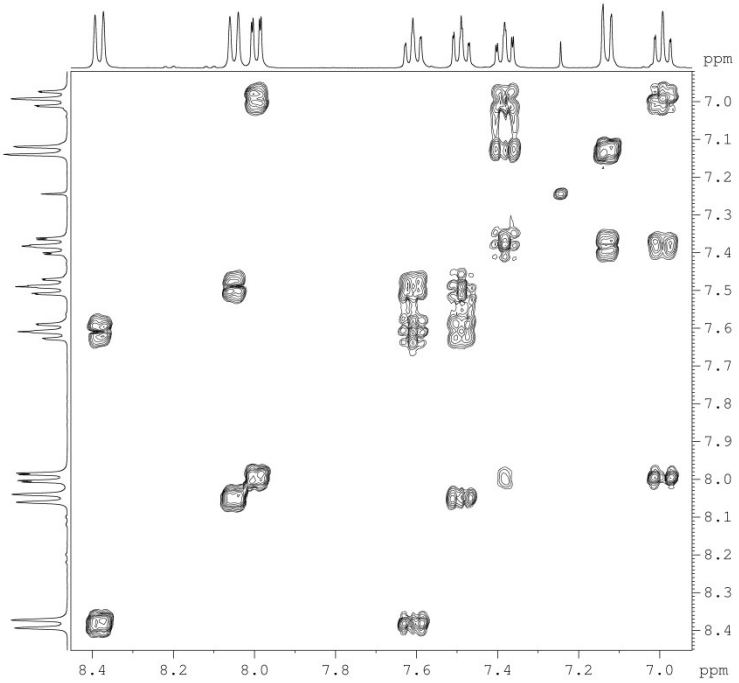

Figure S17. Expanded COSY spectrum of **3** at 400 MHz in $CDCl_3$ (300 K) showing the correlations between aromatic ^1H resonances.

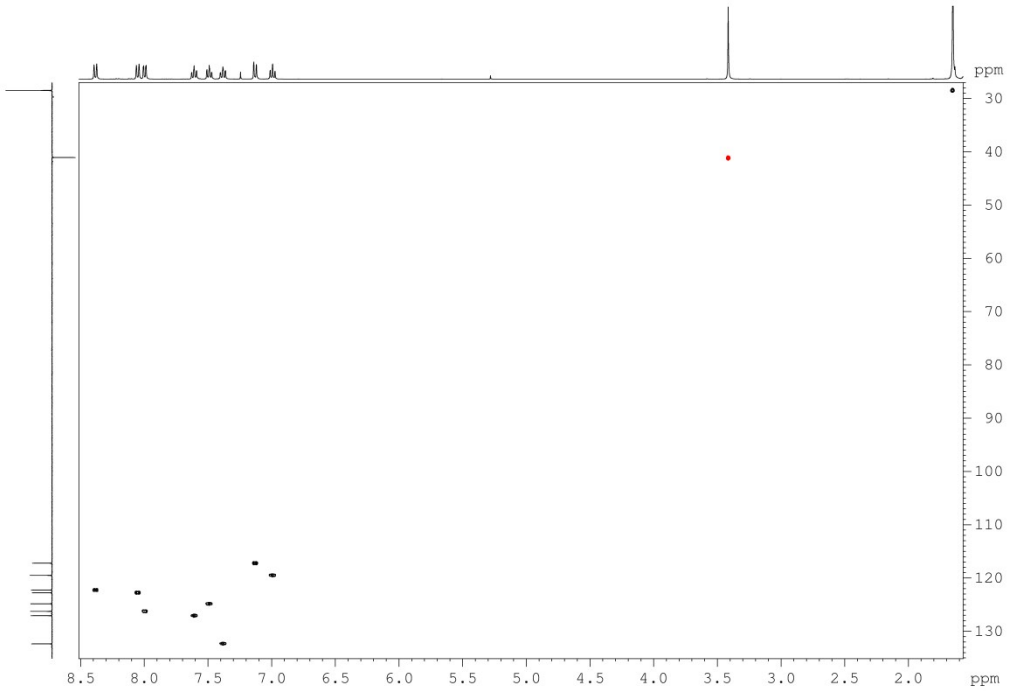

Figure S18. ^{1}H-^{13}C HSQC spectrum of **3** at 400 MHz in $CDCl_3$ (300 K). Correlations in black represent peaks with positive phase (CH_3 and CH correlations) whereas the correlation in red indicates negative intensities (CH_2 correlations).

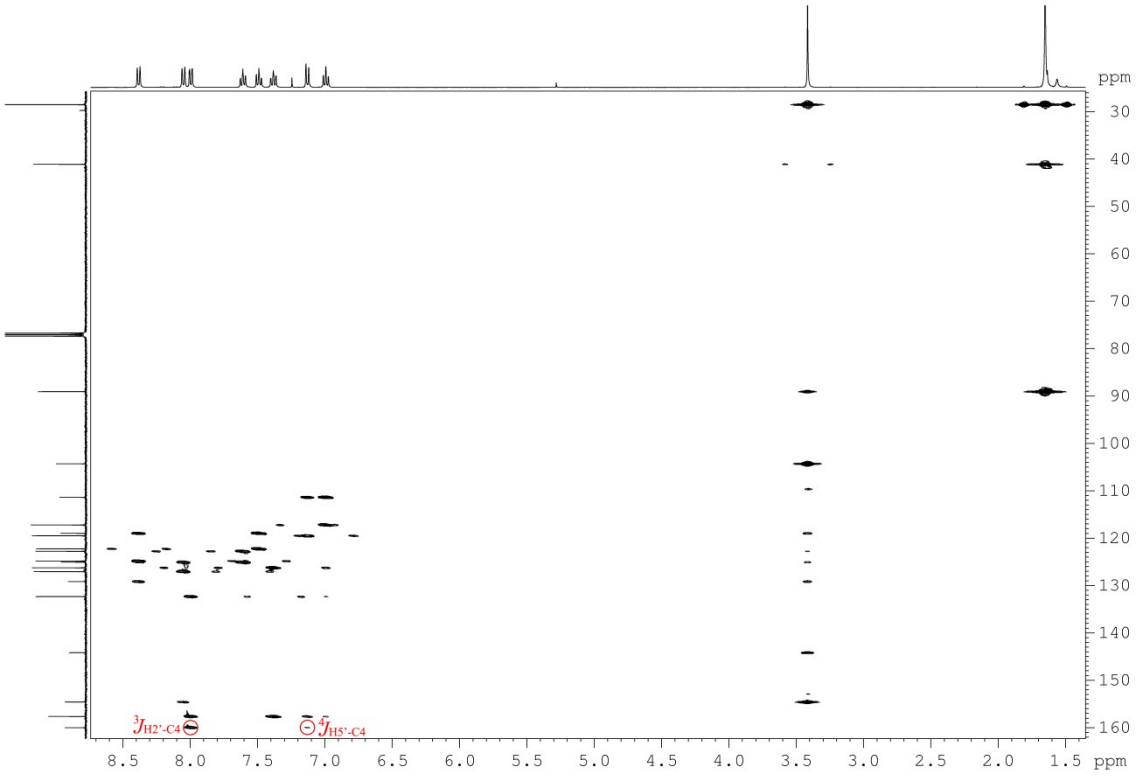

Figure S19. ^{1}H-^{13}C HMBC spectrum of **3** at 400 MHz in $CDCl_3$ (300 K).

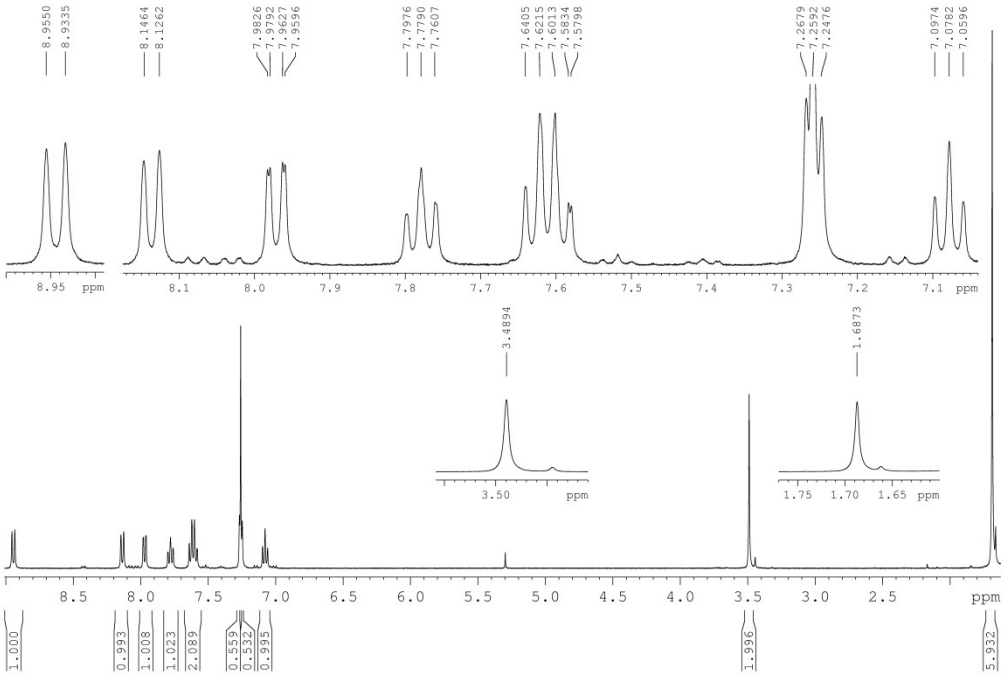

Figure S20. ^{1}H NMR spectrum of **4** at 400 MHz in $CDCl_3$ (300 K).

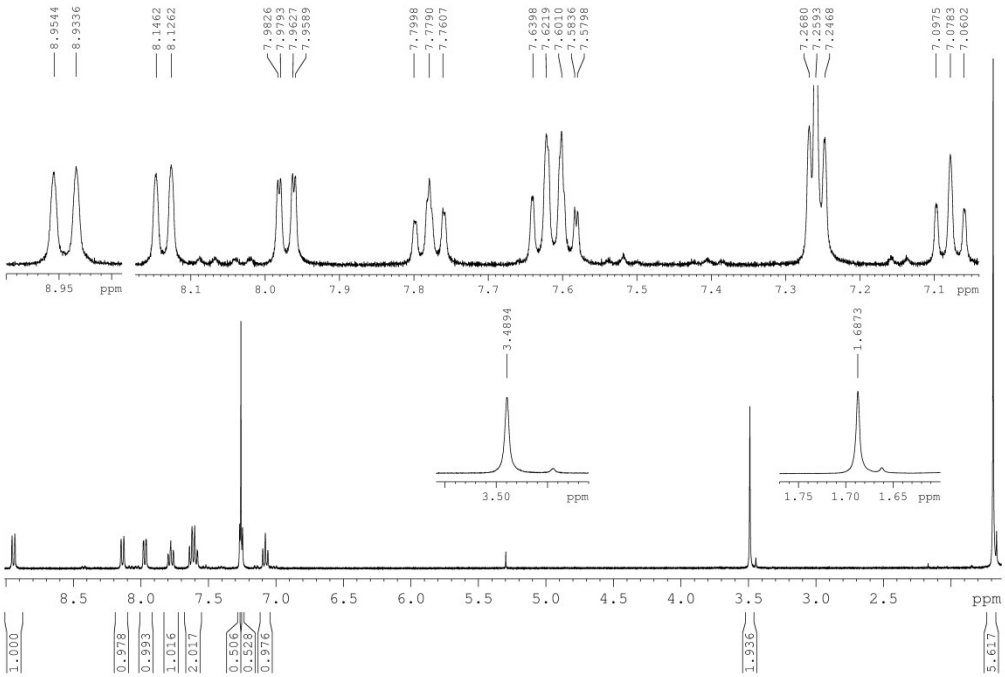

Figure S21. ^{1}H NMR spectrum of **4** at 400 MHz in $CDCl_3$ (300 K). Lorentz-Gauss transformation (lb = -0.3, gb = 30 %).

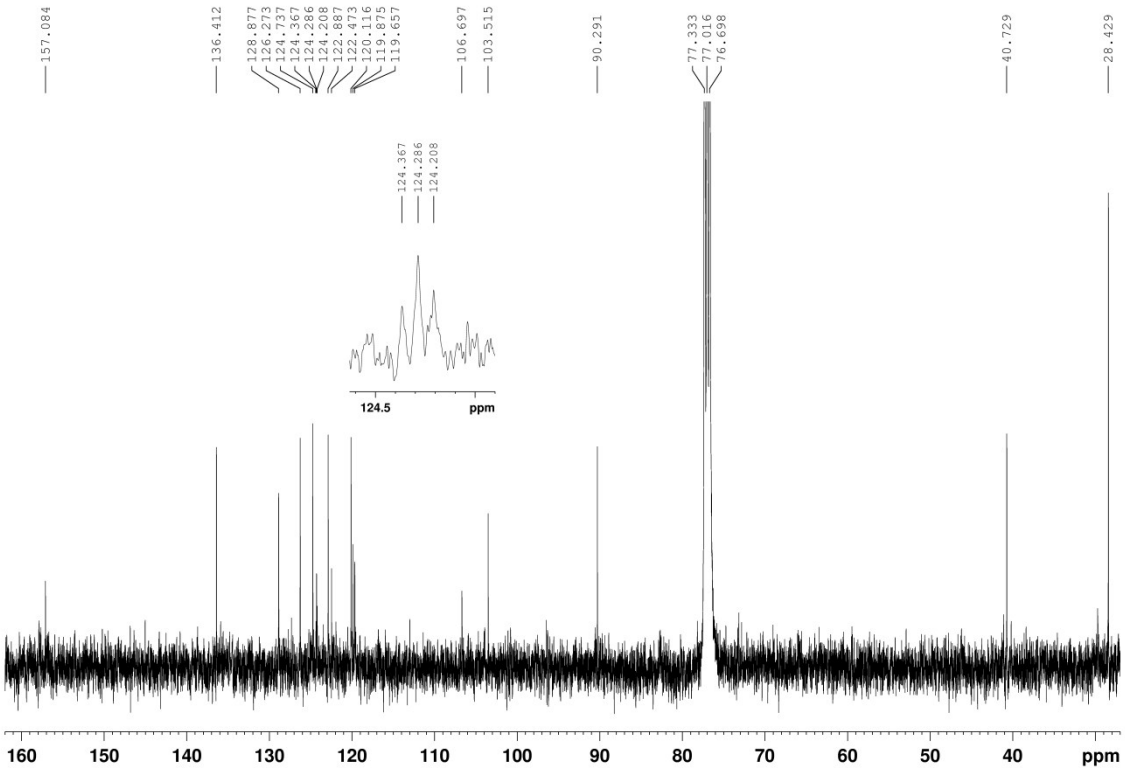

Figure S22. ^{13}C NMR spectrum of **4** at 100 MHz in $CDCl_3$ (300 K).

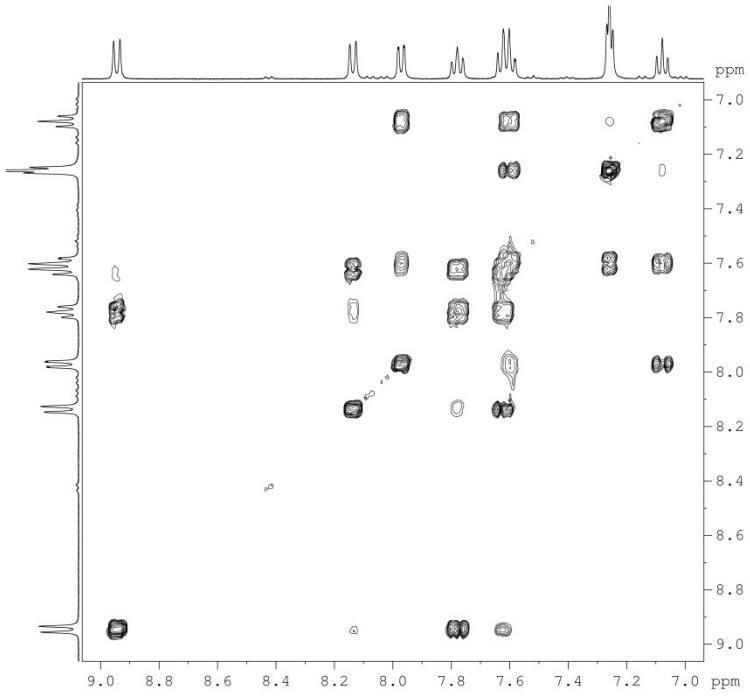

Figure S23. Expanded COSY spectrum of **4** at 400 MHz in $CDCl_3$ (300 K) showing the correlations between aromatic ^1H resonances.

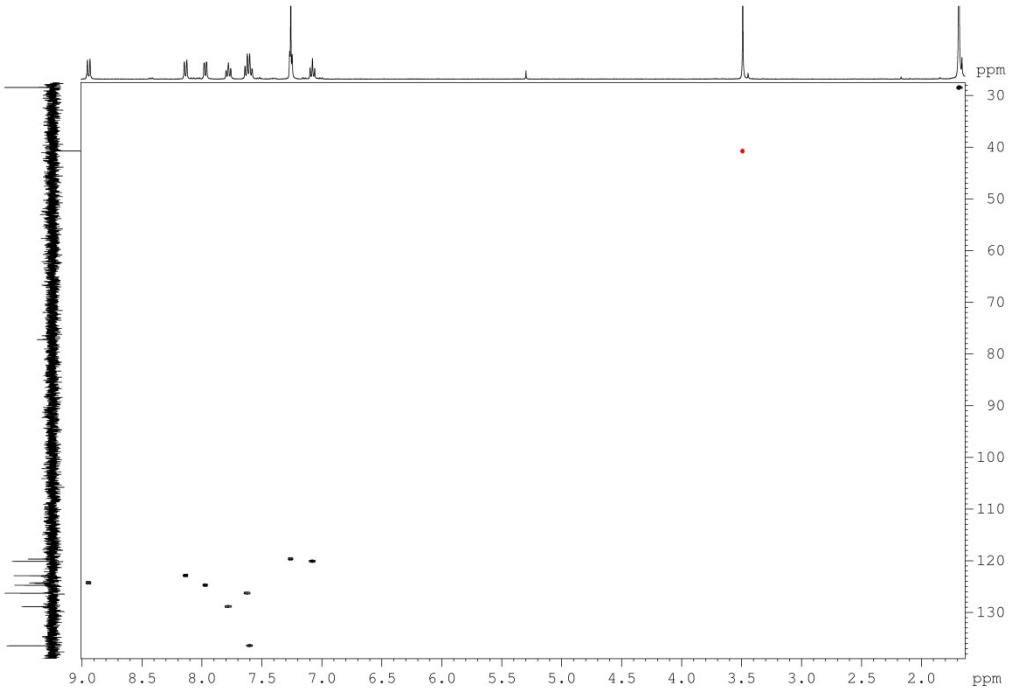

Figure S24. ^{1}H-^{13}C HSQC spectrum of **4** at 400 MHz in $CDCl_3$ (300 K). Correlations in black represent peaks with positive phase (CH_3 and CH correlations) whereas the correlation in red indicates negative intensities (CH_2 correlations).

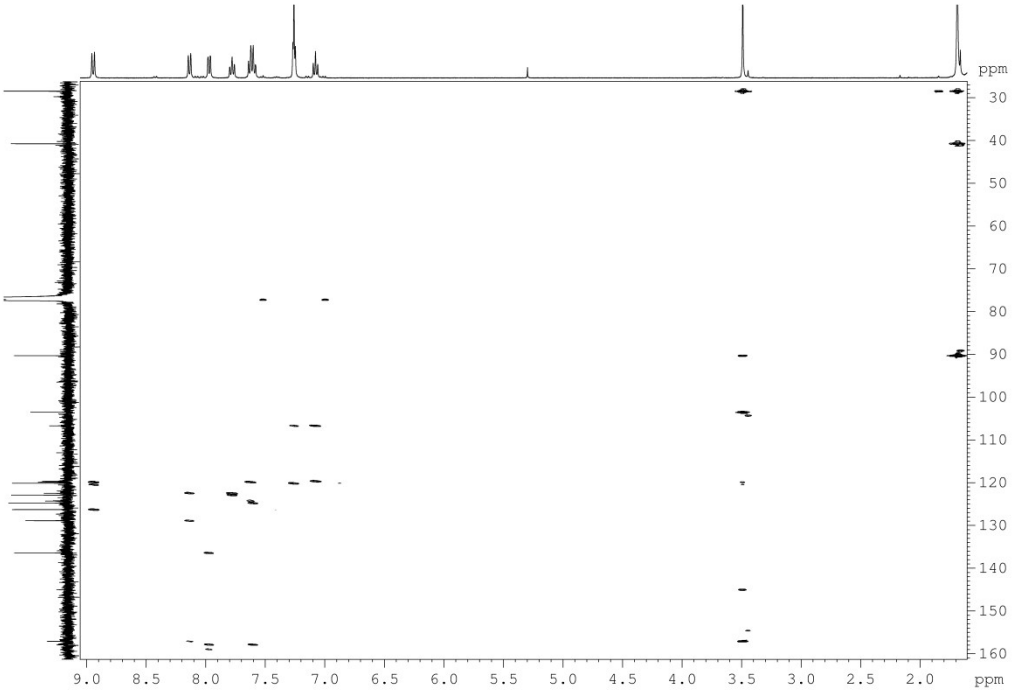

Figure S25. ^{1}H-^{13}C HMBC spectrum of **4** at 400 MHz in $CDCl_3$ (300 K).

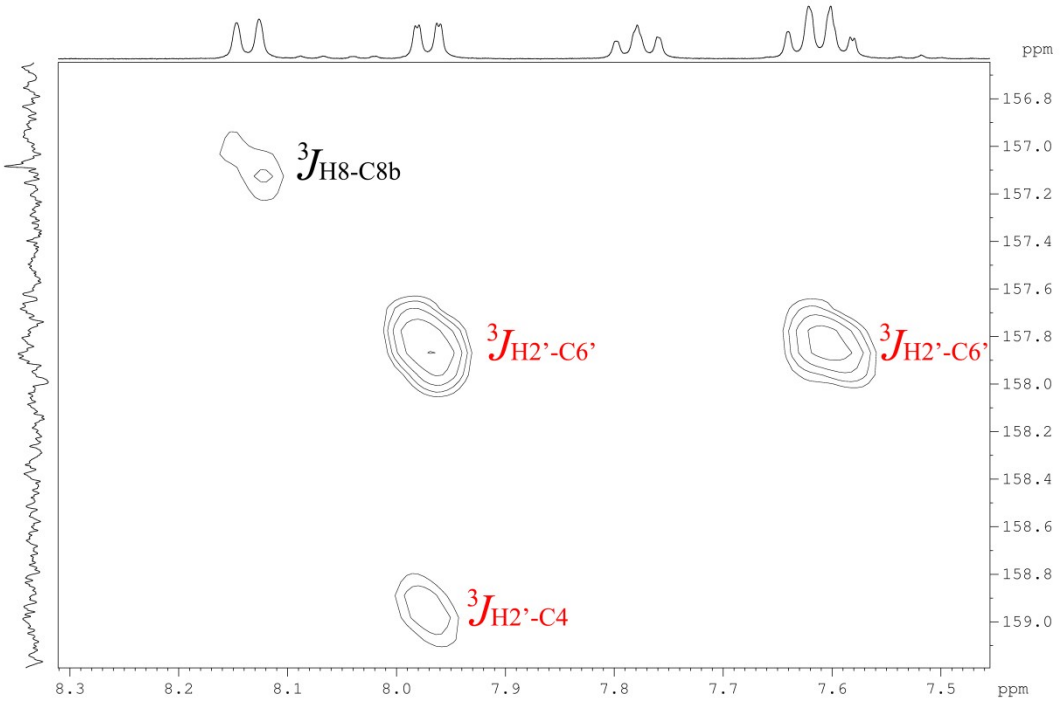

Figure S26. Expanded ^{1}H-^{13}C HMBC spectrum of **4** at 400 MHz in $CDCl_3$ (300 K). The assignments highlighted in red correspond to ^{13}C resonances accessed only through inverse detection HMBC experiment.

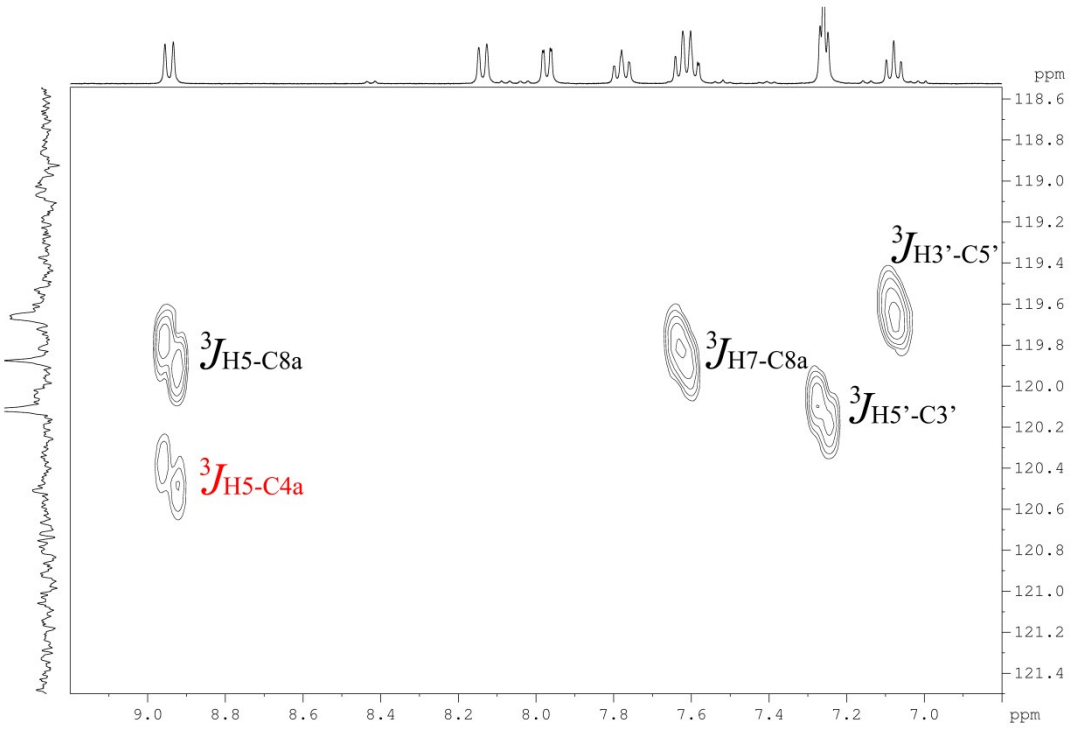

Figure S27. Expanded ^{1}H-^{13}C HMBC spectrum of **4** at 400 MHz in $CDCl_3$ (300 K). The assignment highlighted in red corresponds to the^{13}C resonance accessed only through inverse detection HMBC experiment.

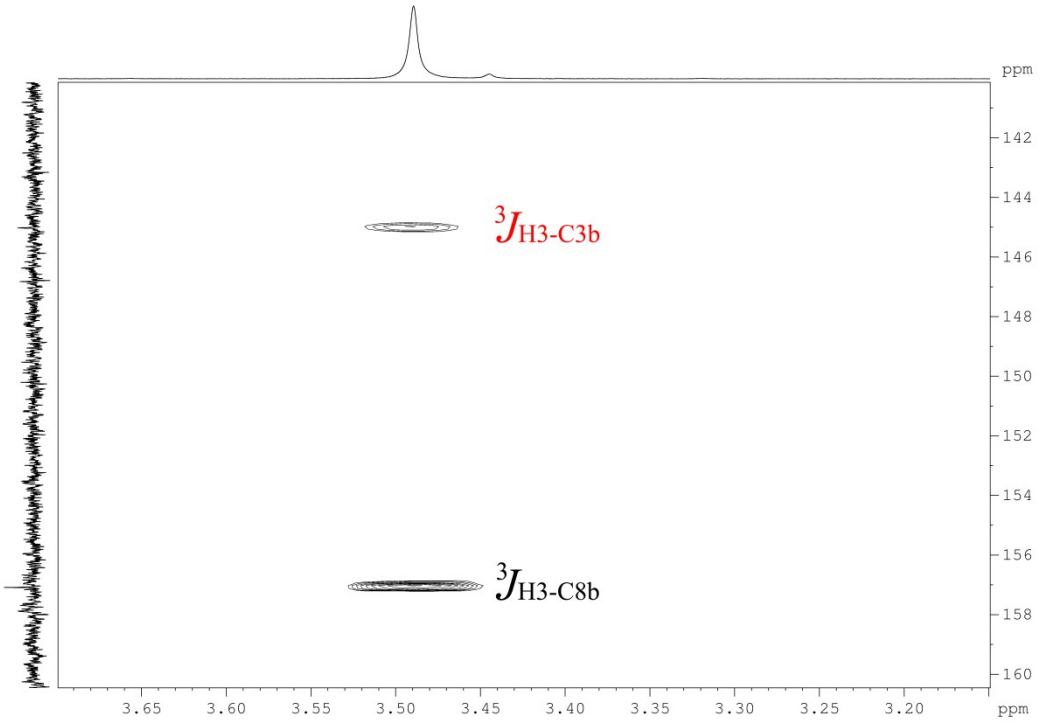

Figure S28. Expanded ^1H-^{13}C HMBC spectrum of **4** at 400 MHz in $CDCl_3$ (300 K). The assignment highlighted in red corresponds to the ^{13}C resonance accessed only through inverse detection HMBC experiment.

HRMS spectra

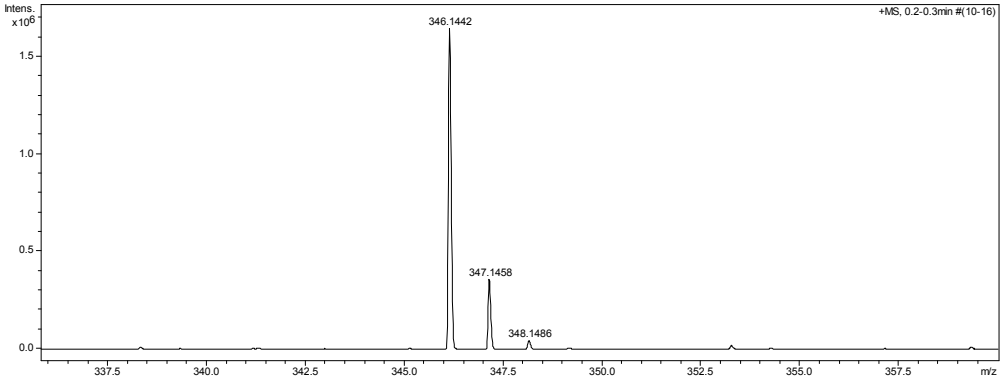

Figure S29. HRMS of compound **1**.

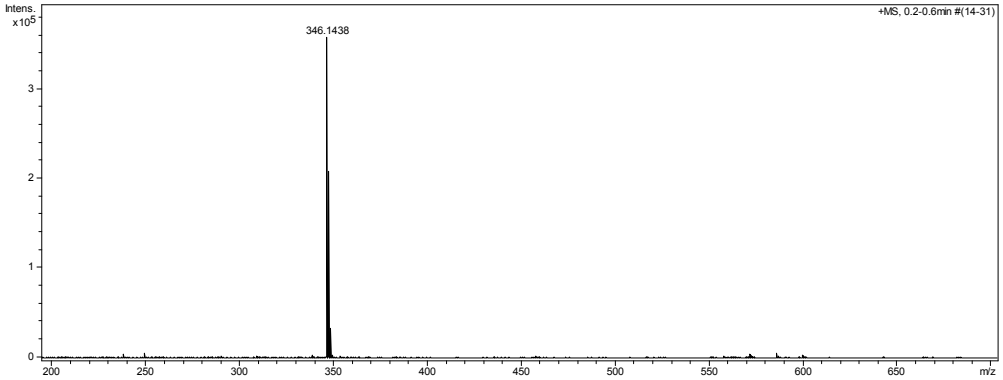

Figure S30. HRMS of compound **2**.

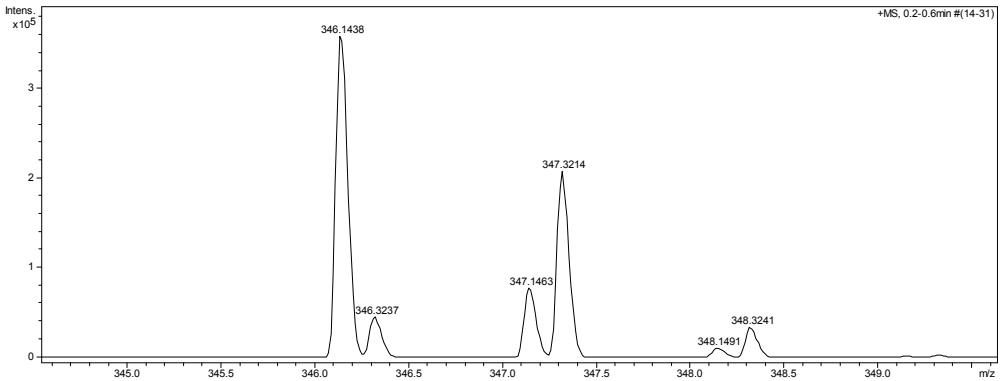

Figure S31. Expanded HRMS of compound **2**.

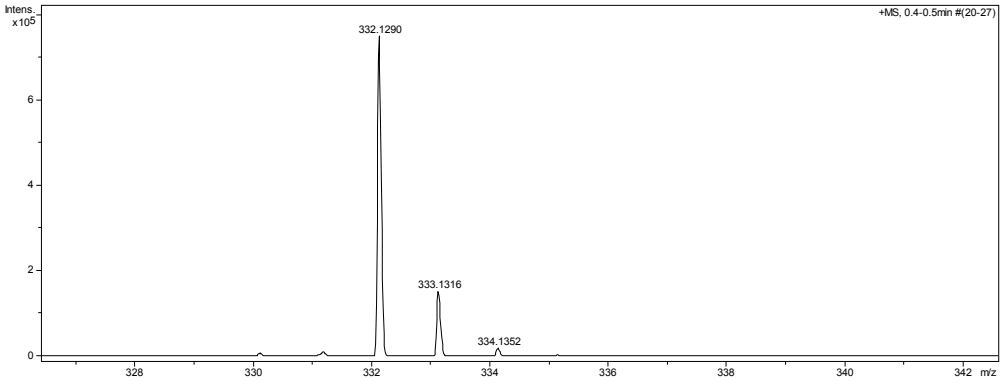

Figure S32. HRMS of compound **3**.

X-ray crystallographic data

X-ray diffraction data collection was performed at room temperature on an Enraf-Nonius Kappa-CCD diffractometer (95 mm CCD camera on κ-goniostat) using graphite monochromated MoK_radiation (0.71073 Å), and on an Agilent–Gemini diffractometer equipped with a CCD area detector using graphite MoKa radiation (0.71073 Å) at 150 K. For Enraf-Nonius Kappa-CCD diffractometer, data collection was carried out using the COLLECT software[10] up to 50° in 2θ. Integration and scaling of the reflections, correction for Lorentz and polarization effects were performed with the HKL DENZO-SCALEPACK[11] system of programs. For Agilent–Gemini diffractometer the CrysAlisPro software package[12] was used for data collection and data reduction. The data was corrected empirically for absorption using spherical harmonics with the SCALE3 ABSPACK[13] scaling algorithm. The structures of the compounds were solved by direct methods with SHELXS-97.[14] The models were refined by full-matrix least squares on F^2 using the SHELXL-97.[15] The program ORTEP-3[16] was used for graphic representation and the program WINGX[17] to prepare material for publication. All H atoms were located by geometric considerations (C–H = 0.93-0.97 Å) and refined as riding with Uiso(H) = 1.5Ueq(C-methyl) or 1.2Ueq(other).

Crystallographic data for the structures were deposited in the Cambridge Crystallographic Data Centre, with numbers CCDC 1030235, 1030236,1030237 and 1033804.

Table S5. Crystal data and structure refinement for the compounds **1** and **2**.

Identification code	Compound **1**		Compound **2**	
Empirical formula	$C_{22}H_{19}NO_3$		$C_{22}H_{18}BF_2NO_3$	
Formula weight	345.38		393.18	
Temperature	293(2) K		293(2) K	
Wavelength	0.71073 Å		0.71073 Å	
Crystal system	orthorrombic		triclinic	
Space group	Pbca		P-1	
Unit cell dimensions	a = 17.7444(2) Å	α = 90°	a = 8.671(2) Å	α = 70.09°
	b = 10.3307(6) Å	β = 90°	b = 10.289(2) Å	β = 88.30°
	c = 18.7617(12) Å	γ = 90°	c = 11.776(2) Å	γ = 68.38°
Volume	3439.2(4) $Å^3$		912.8(2) $Å^3$	
Z	8		2	
Density (calculated)	1.334 Mg/m^3		1.431 Mg/m^3	
Absorption coefficient	0.089 mm^{-1}		0.108 mm^{-1}	
F(000)	1456		408	
Crystal size	0.20 x 0.08 x 0.07 mm^3		0.50 x 0.20 x 0.12 mm^3	
Theta range for data collection	0.992 to 26.4°		1.85 to 29.9°	
Index ranges	-22≤h1≤4, -10≤k≤12, -18≤l≤23		-11≤h≤12, -14≤k≤14, -15≤l≤16	
Reflections collected	12119		15525	
Independent reflections	3515 [R(int) = 0.06]		5276 [R(int) = 0.041]	
Absorption correction	none		none	
Refinement method	Full-matrix least-squares on F^2		Full-matrix least-squares on F^2	
Data / restraints / parameters	2313 / 0 / 269		3312 / 0 / 264	
Goodness-of-fit on F^2	1.055		1.011	
Final R indices [I>2sigma(I)]	R1 = 0.0599, wR2 = 0.0927		R1 = 0.0505, wR2 = 0.0769	
R indices (all data)	R1 = 0.1478, wR2 = 0.1709		R1 = 0.1076, wR2 = 0.1221	
Largest diff. peak and hole	0.33 and -0.24 e.$Å^{-3}$		0.25 and -0.27 e.$Å^{-3}$	

Table S6. Crystal data and structure refinement for the compounds **3** and **4**.

Identification code	Compound **3**		Compound **4**	
Empirical formula	$C_{21}H_{17}NO_3$		$C_{21}H_{16}BF_2NO_3$	
Formula weight	331.4		379.16	
Temperature	293(2) K		293(2) K	
Wavelength	0.71073 Å		0.71073 Å	
Crystal system	monoclinic		orthorrombic	
Space group	P21/c		Pnma	
Unit cell dimensions	a = 10.190(3)Å	α = 90°	a = 13.1646 (4) Å	α = 90°
	b = 9.693(7) Å	β = 106.17°	b = 7.1780 (7) Å	β = 90°
	c = 17.109(2) Å	γ = 90°	c = 17.9760 (8)Å	γ = 90°
Volume	1622.9(2) $Å^3$		1698.7 (2) $Å^3$	
Z	4		8	
Density (calculated)	1.36 Mg/m^3		1.483 Mg/m^3	
Absorption coefficient	0.091 mm^{-1}		0.113 mm^{-1}	
F(000)	696		780	
Crystal size	0.45 x 0.09 x 0.08 mm^3		0.20 × 0.18 × 0.08 mm^3	
Theta range for data collection	2.7 to 26.9°		2.74 to 26.6°	
Index ranges	-9≤h≤10, -9≤k≤8, -17≤l≤15		−17≤h≤16, −-9≤k≤9, −23≤l≤19	
Reflections collected	7553		14547	
Independent reflections	3049 [R(int) = 0.069]		2101 [R_{int} =0.065]	
Absorption correction	none		none	
Refinement method	Full-matrix least-squares on F^2		Full-matrix least-squares on F^2	
Data / restraints / parameters	954 / 0 / 227		1266 /0 / 163	
Goodness-of-fit on F^2	0.917		1.074	
Final R indices [I>2sigma(I)]	R1 = 0.042, wR2 = 0.092		R1 = 0.066, wR2 = 0.1258	
R indices (all data)	R1 = 0.086, wR2 = 0.10		R1 = 0.1409, wR2 = 0.1720	
Largest diff. peak and hole	0.28 and -0.23 e.$Å^{-3}$		0.358 and -0.300 e.$Å^{-3}$	

The crystal packing of **1** showed π-π stacking interactions between centroids of oxazole (C7-N1-C8-C17-O2) and aryl (C1-C6) rings, bond distance d(Cg1-Cg2) = 3.321(2) Å and symmetry operation (½-x, ½+y,z). In the packing of this compound, molecules form crossed layers that extend along the crystallographic direction [100] and are parallel to planes (024) and (0-24), respectively. In the packing of **2**, molecules form chains that extend parallel to [42-3] direction. These chains are linked by intermolecular interactions C18-H18b···F2 [d(H18b···F2) = 2.43(2) Å, \(C18H18b···F2) = 150(2)°, symmetry operation (-x,-y,-z+1)] and C21-H21c···F1 [d(H21c···F1) = 2.35(3) Å, \(C21H21c···F1) = 170(4)°, symmetry operation (x-1,y+1,z)]. The packing of **4** shows a perfect order where molecules are positioned on the symmetry operators at 1/4 and 3/4 of the b axis of the unit cell. Intermolecular interactions C3-H3···O1 [d(H3···O1) = 2.51(2) Å, \(C3H3···O1) = 178(3)°, symmetry operation (x-1,y,z)] and C12-H12···B [d(H12···B) = 3.14(2) Å, \(C12H12···B) = 135(3)°, symmetry operation (-1/2+x,1/2-y,1/2-z)] link the molecules forming chains that extend along [100] direction.

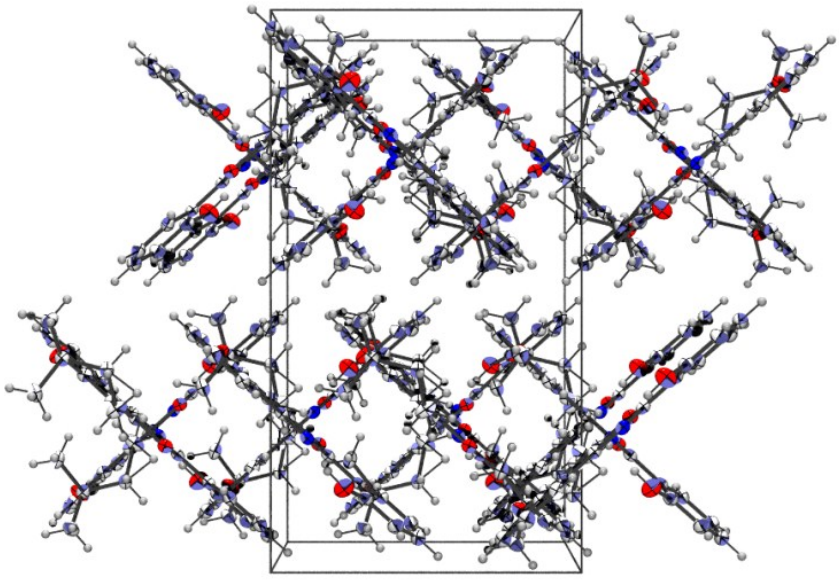

Figure S33. Crystal packing of compound **1**.

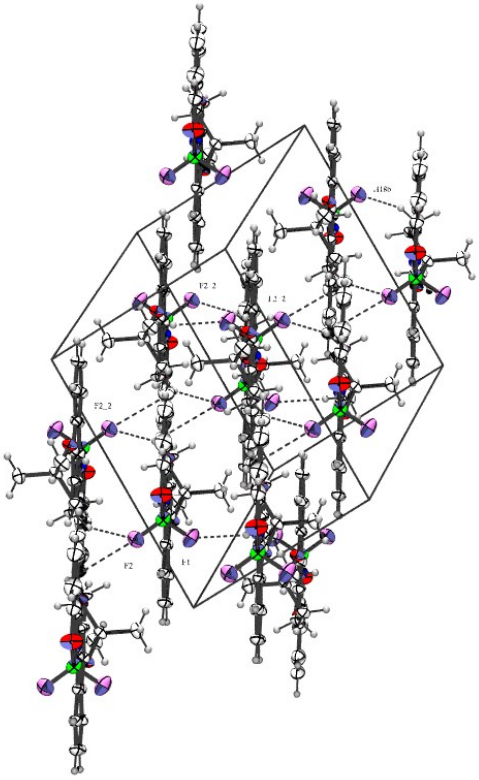

Figure S34. Crystal packing of compound **2**.

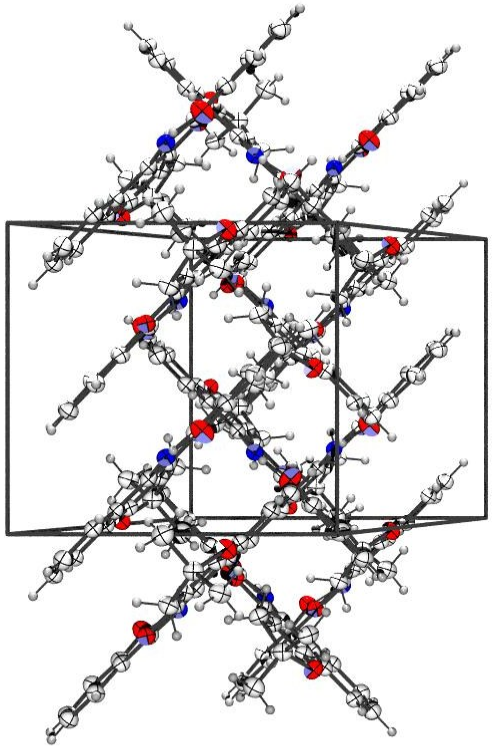

Figure S35. Crystal packing of compound **3**. View along de [100] direction.

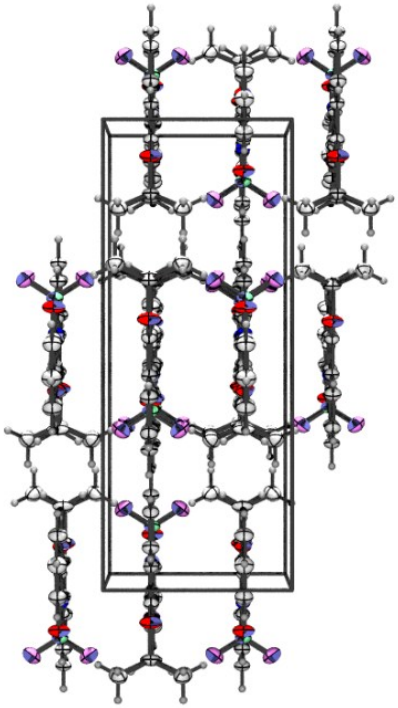

Figure S36. Crystal packing of compound **4**. View along de [100] direction.

Photophysical Parameters

Absorption spectra were obtained on a Varian Cary 100 spectrophotometer at room temperature in the solvents described below. Steady state fluorescence spectra were obtained on a Varian Cary Eclipse spectrofluorimeter with a xenon arc lamp as the light source while using an excitation wavelength (λ_{exc}) corresponding to a higher absorption band. In all experiments, a quartz cuvette was employed with a 1 cm optical path length. The absorbance and fluorescence emission for all of the compounds in seven different solvents with distinct polarities (ethyl acetate, acetonitrile, dichloromethane, hexane, toluene, methanol, and dimethyl sulfoxide) were measured.

In studies on solvatochromism for each component tested, and for each solvent tested, a dichloromethane solution of the initial concentration of 5.00 x 10^{-6} mol L^{-1} was prepared and an aliquot of 200 x 10^{-6} L was moved into a 10.0 mL volumetric flask. After the dichloromethane had completely evaporated, the volume of the balloon was completed with one of the tested solvents. For each sample in different solvents, the absorption and emission spectra were recorded.

Molar absorption and emission coefficients (ε) were obtained in dichloromethane. The absorbance of five solutions of known concentrations of **1**, **2**, **3** and **4** were obtained and plotted against the respective concentration, and ε was calculated from the slope of the regression analyses of the plotted data.

The respective calibration curves were built up for each molecule studied by absorption and emission spectroscopies. Solutions with 6.0; 7.5; 9.0; 10.5 and 12.0x10^{-6} mol L^{-1} concentrations were prepared. For complex **2**, the following concentrations were prepared: 1.5; 2.5; 3.5; 4.5 and 5.5 10^{-6} mol L^{-1}.

Quantum yields were obtained by a comparative method[18] using 500 x 10^{-6} mol L^{-1} quinine sulfate in 0.1 mol L^{-1} and H_2SO_4 (aq) as standard[19] ($\varphi = 0.54$[20]). The emission spectra from four samples of each fluorophore (absorbance between 0.4 and 0.05 at the excitation wavelength) were obtained. The results were plotted with the integrated fluorescence intensity vs. absorbance to obtain the slope of the curve. A curve was obtained for each tested compound as well as for the standard. The quantum yield of the tested compound (Φ_x) was calculated using the following formula, where Φ_{St} is the quantum yield of the standard, m_x and m_{St} are the slopes for the test compound and standard compound, respectively, and n_x and n_{st} are the refractive indexes of the solvents.

$$\Phi_X = \Phi_{St}\left[\frac{m_x}{m_{St}}\right]\left[\frac{n_x}{n_{St}}\right]^2 \qquad (1)$$

Photophysical properties of the oxazoles (**1** and **3**) and their boron complexes (**2** and **4**) were studied in seven solvents, which varied in polarity and were either protic or aprotic: ethyl acetate, hexane, dichloromethane, acetonitrile, dimethyl sulfoxide, methanol and toluene. The four studied compounds, regardless of the solvent, showed strong absorptions in the ultraviolet (300-400 nm) as well as strong fluorescent emissions, which are visible to the naked eye, in the blue region (400-500 nm) (Figure S37). UV-VIS absorption wavelength and fluorescence emission intensities as a function of the pH (2–13) were also determined (Figure S40).

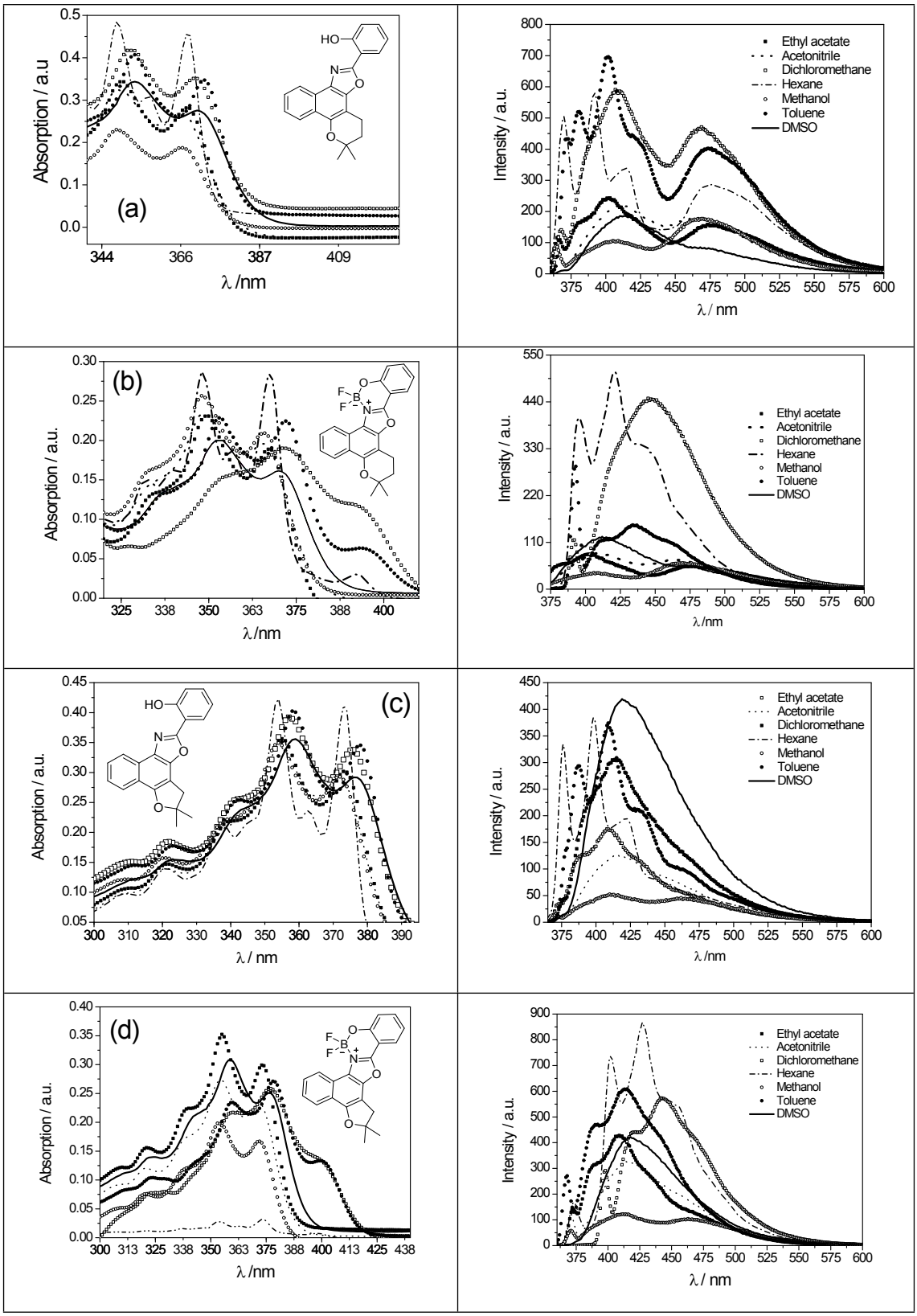

Figure S37. Absorption spectra (left) and emission spectra (right) of (a) **1**, (b) **2**, (c) **3** and (d) **4** in different solvents.

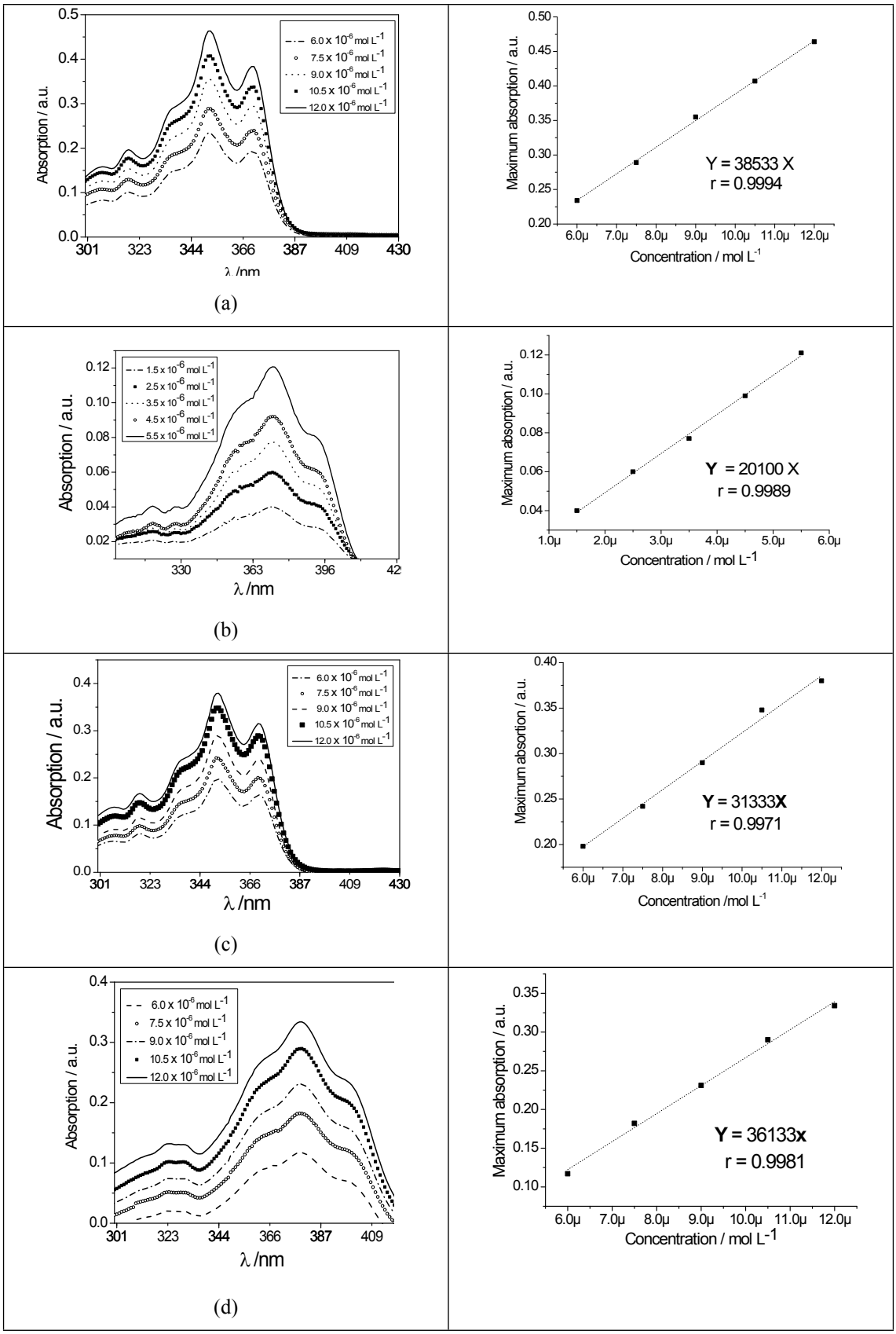

Figure S38. Absorption spectra (left) and calibration curve (right) for (a)**1**, (b)**2**, (c)**3** and (d)**4**.

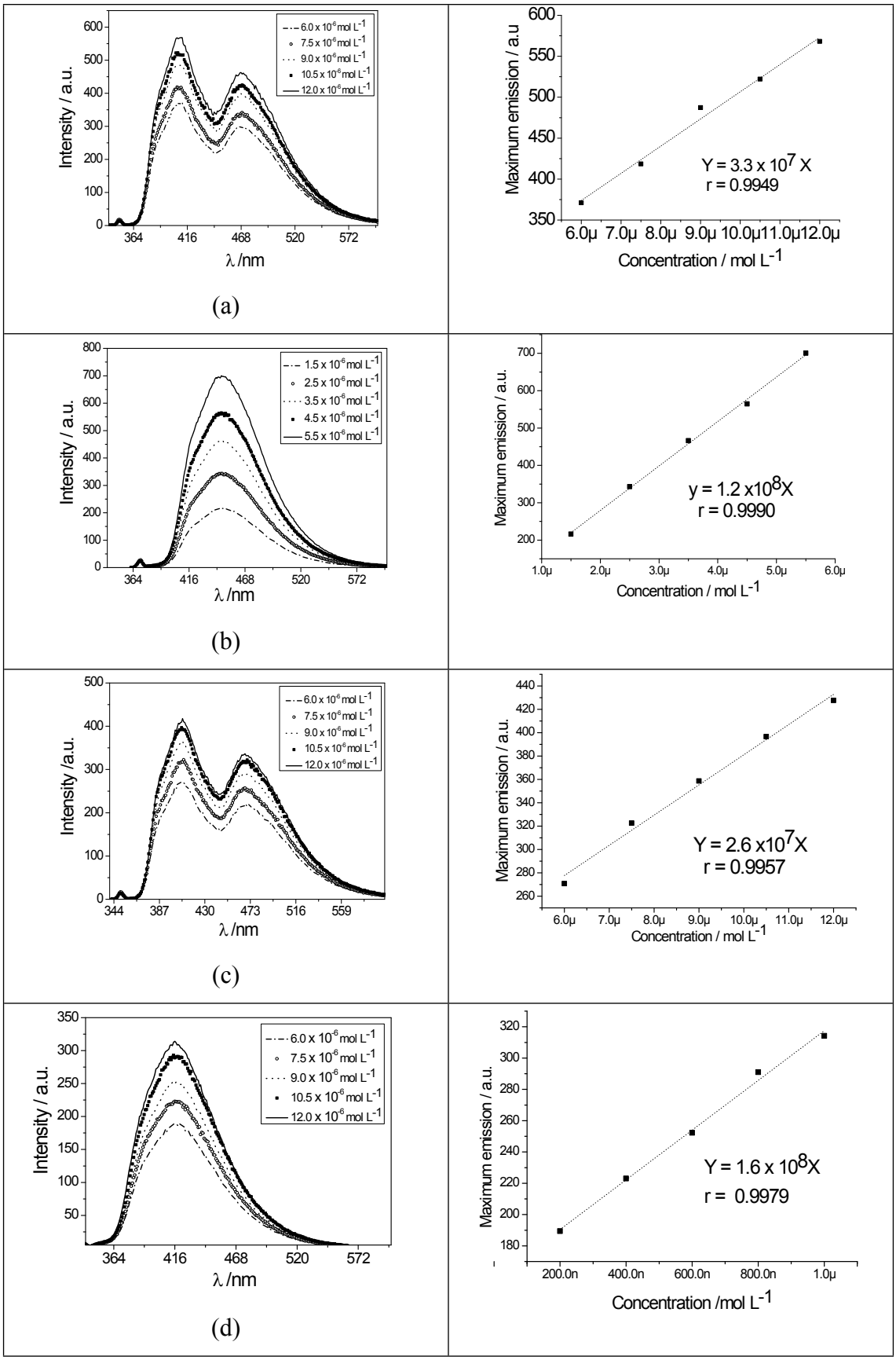

Figure S39. Emission spectra (left) and calibration curve (right) obtained for (a)**1**, (b)**2**, (c)**3** and (d)**4**.

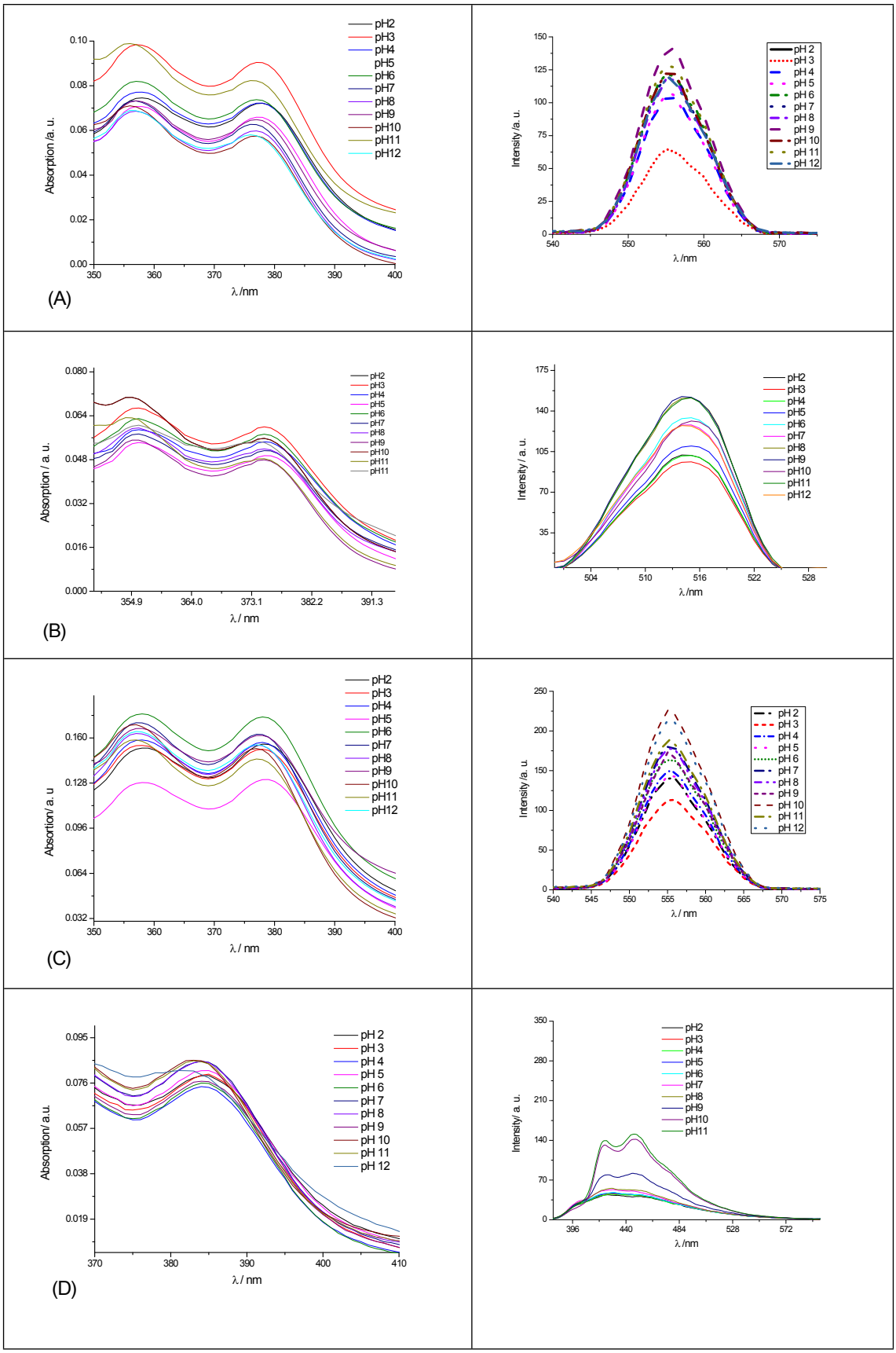

Figure S40. UV-VIS absorption wavelength (right) and fluorescence emission intensity (left) as a function of pH (2–12) obtained for (a)**1**, (b)**2**, (c)**3** and (d)**4**.

Table S7. UV-Vis and fluorescence emission data (in different solvents) for **1**, **2**, **3** and

4 (10 μM of concentration).

Compound	Solvent	λ_{max} (abs) (nm)	λ_{max} (em) (nm)	Stokes shift (nm)
1	Hexane	348	396	48
	CH_3Ph	353	402	49
	CH_2Cl_2	351	407	56
	EtOAc	350	403	53
	MeOH	348	470	122
	MeCN	348	412	64
	DMSO	353	414	61
2	Hexane	348	421	73
	CH_3Ph	353	433	80
	CH_2Cl_2	371	445	74
	EtOAc	350	477	127
	MeOH	348	469	121
	MeCN	348	461	113
	DMSO	352	412	60
3	Hexane	354	398	44
	CH_3Ph	358	409	51
	CH_2Cl_2	357	414	57
	EtOAc	355	408	53
	MeOH	354	410	56
	MeCN	354	416	62
	DMSO	359	419	60
4	Hexane	373	427	54
	CH_3Ph	378	445	67
	CH_2Cl_2	377	442	65
	EtOAc	355	411	56
	MeOH	355	412	57
	MeCN	355	422	67
	DMSO	359	417	58

The quantum yields measured in triplicate with the respective standard deviations are 0.80 ± 0.07, 0.58 ± 0.05, 0.61 ± 0.05 and 0.42 ± 0.03.

Computational details

Theoretical treatment of all DTD compounds was performed using the density functional theory (DFT) approach of the Gaussian 09 series of programs.[21] Geometry optimization of the ground (S_0) and first excited (S_1) states (in DMSO) were conducted with 6-31+g(d) Pople's split-valence basis set and hybrid exchange–correlation functional using the Coulomb-attenuating method (CAM-B3LYP).[22] Harmonic frequency calculations were performed to verify whether we have located a genuine minimum or not. The optimized geometries of S_0 and S_1 were employed for the single point TD-DFT calculation using different exchange-correlation (XC) functional (B3LYP, CAM-B3LYP, M062X, wB97XD, PBE1PBE and B2PLYP) in combination with a large 6-311+G(2d,p) basis set. In particular, absorption spectra in close agreement with experiments have been obtained using the 6-311+G(2d,p) basis set.[23] To include the solvent effects in our quantum mechanics calculations, we have employed the self-consistent reaction field (SCRF) approach with the polarizable continuum model (PCM)[24], where the solute molecule is enclosed in a cavity embedded in a dielectric medium.

Table S8. Selected theoretical calculated data for the compounds **1**, **2**, **3** and **4** in their

ground and first excited states obtained from different exchange-correlation (*XC*) functionals (B3LYP, CAM-B3LYP, M062X, wB97XD, PBE1PBE and B2PLYP) using the large 6-311+g(2d,p) Pople's split-valence basis set. All results were obtained using the geometries fully optimized at CAM-B3LYP/6-31+g(d) level of calculation.

Compounds	*XC*	State	μ(D)	HOMO(eV)	LUMO(eV)	$\Delta E_{HOMO-LUMO}$(eV)
1	**B3LYP**	S_0	12.8217	-5.595751501	-1.758400418	-3.837351083
		S_1	11.3451	-5.270303203	-2.108066858	-3.162236344
	CAM-B3LYP	S_0	8.992	-6.835774822	-0.639467809	-6.196307013
		S_1	9.8709	-6.421073145	-1.066958842	-5.354114303
	M062X	S_0	9.081	-6.784345284	-0.94042585	-5.843919433
		S_1	9.8771	-6.365834011	-1.360569807	-5.005264205
	wB97XD	S_0	8.306	-7.3693903	-0.044082462	-7.325307839
		S_1	9.389	-6.948430002	-0.479192686	-6.469237316
	PBE1PBE	S_0	12.0953	-5.79766006	-1.63350011	-4.16415995
		S_1	11.1551	-5.455340697	-1.996772248	-3.458568448
	B2PLYP	S_0	9.1409	-6.310322763	-0.376061495	-5.934261268
		S_1	10.0234	-5.871675057	-0.826137987	-5.045537071
2	**B3LYP**	S_0	17.8929	-5.885552869	-2.209021138	-3.676531731
		S_1	16.6811	-5.603370692	-2.561952946	-3.041417746
	CAM-B3LYP	S_0	14.0333	-7.131834812	-1.095530808	-6.036304004
		S_1	15.1165	-6.770467472	-1.523293955	-5.247173516
	M062X	S_0	14.111	-7.088296578	-1.388053317	-5.700243262
		S_1	15.0407	-6.72366387	-1.813095324	-4.910568546
	wB97XD	S_0	13.2843	-7.66681086	-0.494703182	-7.172107679
		S_1	14.6248	-7.299729126	-0.926820152	-6.372908974
	PBE1PBE	S_0	17.3425	-6.091815252	-2.085209286	-4.006605966
		S_1	16.5616	-5.794666806	-2.451202564	-3.343464243
	B2PLYP	S_0	14.4992	-6.618355767	-0.836750431	-5.781605336
		S_1	15.4808	-6.233314512	-1.288731721	-4.944582791
3	**B3LYP**	S_0	12.0944	-5.541328708	-1.78670027	-3.754628438
		S_1	10.3941	-5.226764969	-2.12602638	-3.100738589
	CAM-B3LYP	S_0	8.3044	-6.776726093	-0.672121484	-6.104604608
		S_1	8.9472	-6.37127629	-1.089544301	-5.281731989
	M062X	S_0	8.4207	-6.726112896	-0.973623754	-5.752489142
		S_1	8.9927	-6.31630927	-1.384243721	-4.932065549
	wB97XD	S_0	7.6896	-7.308164659	-0.077824593	-7.230340066
		S_1	8.4997	-6.897000464	-0.502866601	-6.394133863
	PBE1PBE	S_0	11.3848	-5.739427672	-1.66370476	-4.075722913
		S_1	10.2226	-5.408264981	-2.016364453	-3.391900528
	B2PLYP	S_0	8.2941	-6.257260541	-0.408170942	-5.849089599
		S_1	8.9967	-5.823238772	-0.843281166	-4.979957606
4	**B3LYP**	S_0	17.4279	-5.827048368	-2.228069115	-3.598979252
		S_1	15.9842	-5.553301723	-2.569844251	-2.983457472
	CAM-B3LYP	S_0	13.5516	-7.069520715	-1.118660495	-5.95086022
		S_1	14.4358	-6.71468411	-1.535539084	-5.179145026
	M062X	S_0	13.6526	-7.026254595	-1.411727231	-5.614527364
		S_1	14.4046	-6.667880508	-1.825612566	-4.842267942
	wB97XD	S_0	12.8316	-7.602047737	-0.518921324	-7.083126413
		S_1	13.9672	-7.242040967	-0.940697964	-6.301343002
	PBE1PBE	S_0	16.9199	-6.029229041	-2.105617833	-3.923611208
		S_1	15.8956	-5.740516128	-2.460454438	-3.28006169
	B2PLYP	S_0	13.8571	-6.562300291	-0.85933589	-5.702964401
		S_1	14.6998	-6.181884973	-1.299888393	-4.88199658

Table S9. Selected theoretical TD-DFT results for the compounds **1**, **2**, **3** and **4** obtained from different exchange-correlation (*XC*) functionals (B3LYP, CAM-B3LYP, M062X, wB97XD, PBE1PBE and B2PLYP) using the large 6-311+g(2d,p) Pople's split-valence basis set. All results were obtained using the geometries fully optimized at CAM-B3LYP/6-31+g(d) level of calculation.

Compounds	*XC*	**Orbital Composition (Major contributions)**	**Oscillator Strength**	**Wavelength (nm)**
1	**B3LYP**	HOMO->LUMO (99%)	1.0117	377.170043318
	CAM-B3LYP	HOMO->LUMO (91%)	1.1529	333.091549727
	M062X	HOMO->LUMO (92%)	1.168	330.032572842
	wB97XD	HOMO->LUMO (88%)	1.163	328.999168474
	PBE1PBE	HOMO->LUMO (98%)	1.0585	364.968168849
	B2PLYP	HOMO->LUMO (91%)	1.1788	326.323463283
2	**B3LYP**	HOMO->LUMO (99%)	0.8787	396.784768584
	CAM-B3LYP	HOMO->LUMO (87%)	1.0787	344.752486276
	M062X	HOMO->LUMO (89%)	1.098	341.26985037
	wB97XD	HOMO->LUMO (83%)	1.0953	339.698987998
	PBE1PBE	HOMO->LUMO (98%)	0.9338	382.122100227
	B2PLYP	HOMO->LUMO (89%)	1.1177	334.981456391
3	**B3LYP**	HOMO->LUMO (99%)	0.9721	385.89229867
	CAM-B3LYP	HOMO->LUMO (91%)	1.1035	339.987760549
	M062X	HOMO->LUMO (93%)	1.1201	336.838015213
	wB97XD	HOMO->LUMO (88%)	1.1092	335.834380626
	PBE1PBE	HOMO->LUMO (98%)	1.0137	373.533793202
	B2PLYP	HOMO->LUMO (91%)	1.1308	332.91267021
4	**B3LYP**	HOMO->LUMO (99%)	0.8423	405.890580238
	CAM-B3LYP	HOMO->LUMO (88%)	1.0544	350.730796717
	M062X	HOMO->LUMO (90%)	1.0716	347.311716734
	wB97XD	HOMO->LUMO (84%)	1.0737	345.386346044
	PBE1PBE	HOMO->LUMO (98%)	0.8953	390.868022193
	B2PLYP	HOMO->LUMO (89%)	1.0926	340.669716545

Cartesian coordinates of the calculated structures

Compound 1 - S_0 - DMSO

C	-4.51868700	0.51230500	0.04780600
C	-3.53317800	-0.49591400	-0.00044500
C	-3.92114000	-1.84135700	-0.03130500
C	-5.25827300	-2.19204000	-0.01519400
C	-6.22896500	-1.18877500	0.03274100
C	-5.86665100	0.14697500	0.06380400
C	-2.13619200	-0.11099400	-0.01718200
N	-1.66655500	1.10303200	0.00785200
C	-0.28617300	0.95719400	-0.02463300
C	0.00741400	-0.38217600	-0.06769700
O	-1.17538500	-1.07217100	-0.06289700
C	0.76056300	1.91559900	-0.02624300
C	2.08597400	1.40160600	-0.06750000
C	2.31887900	-0.02204100	-0.11281700
C	1.29368000	-0.94330700	-0.11942800
O	3.62501400	-0.38407500	-0.16980500
C	3.97441800	-1.77255200	0.07748600
C	1.54640900	-2.42183900	-0.20252300
C	2.98122400	-2.67587900	-0.65583200
C	3.97440600	-2.00103300	1.58666900
C	5.37391900	-1.91845200	-0.49667300
C	3.16423300	2.31552800	-0.06301300
C	2.93620000	3.66950800	-0.02423700
C	1.61990800	4.17110300	0.01334000
C	0.55073600	3.30970100	0.01343000
H	-3.15252800	-2.60517700	-0.06832500
H	-5.54832000	-3.23607200	-0.03946100
H	0.84101100	-2.88091000	-0.90138500
H	1.35792400	-2.89078600	0.77006400
H	3.06956300	-2.47599500	-1.72856800
H	3.25830500	-3.72083500	-0.49569600
H	2.99705000	-1.79108400	2.02599300

H	4.23582300	-3.03804100	1.81233000
H	4.70859800	-1.34739900	2.06312600
H	6.05699300	-1.21327700	-0.01703100
H	5.37017800	-1.72372700	-1.57171000
H	5.74734600	-2.93101400	-0.32713800
H	4.17433900	1.92617700	-0.08945700
H	3.77404200	4.35867100	-0.02080900
H	1.45263500	5.24266900	0.04392700
H	-0.46671900	3.68441800	0.04395400
O	-4.21442500	1.82157000	0.07928000
H	-3.23211100	1.91982900	0.06271600
H	-6.61111600	0.93426600	0.10084900
H	-7.28097600	-1.45449500	0.04571600

Compound 2 - S_0 - DMSO

C	-4.18232500	-0.20545700	0.06872600
C	-3.16958700	-1.18122000	0.00481800
C	-3.48733400	-2.54659200	-0.03690000
C	-4.80757400	-2.94306200	-0.01475400
C	-5.81684400	-1.97315900	0.05222100
C	-5.51676700	-0.62415300	0.09424300
O	-3.90570800	1.09543700	0.11724500
C	-1.82810000	-0.69089100	-0.00003200
N	-1.49561600	0.58182200	0.02536300
C	-0.09494800	0.63693300	0.00731500
C	0.33682800	-0.66269400	-0.03275200
O	-0.76291800	-1.49137300	-0.03191000
C	0.84678500	1.70304200	0.00381700
C	2.21607500	1.31340300	-0.05448200
C	2.59364500	-0.07888800	-0.09849600
C	1.66679000	-1.09782500	-0.08986100
O	3.92360900	-0.30790300	-0.16803400
C	4.41788300	-1.65855900	0.05797000
C	2.06015900	-2.54467900	-0.17702000
C	3.50374900	-2.65224500	-0.66016700
C	4.47631800	-1.89231600	1.56480100
C	5.81027600	-1.65591100	-0.55029400
C	3.20874200	2.31859300	-0.06602200
C	2.86440200	3.64657200	-0.02353500
C	1.51064400	4.02469800	0.04331300
C	0.51855600	3.07554300	0.06034800
B	-2.59870800	1.71899600	-0.02425300
F	-2.38036100	2.59368700	1.02446200
F	-2.48545900	2.37100600	-1.23672000
H	-2.68589400	-3.27528700	-0.08588900
H	-5.06273300	-3.99554100	-0.04777000
H	1.39089200	-3.07212700	-0.86267700
H	1.93906800	-3.02755100	0.79909400

H	3.54929200	-2.44236700	-1.73356000
H	3.88610100	-3.66468600	-0.50996100
H	4.84981000	-2.89748900	1.77618000
H	3.49333100	-1.78870200	2.02913200
H	5.14948000	-1.16812700	2.02902500
H	6.43005900	-0.88990000	-0.07827500
H	5.76038200	-1.45275200	-1.62252400
H	6.28818700	-2.62693400	-0.40140500
H	4.24761000	2.01730200	-0.10727800
H	3.63755200	4.40728200	-0.03383900
H	1.24734000	5.07617400	0.08868000
H	-0.51866400	3.36969600	0.14139100
H	-6.85627200	-2.28392400	0.07040500
H	-6.29442100	0.12887900	0.14536800

Compound 3 - S_0 - DMSO

C	-4.29286200	0.58998500	0.02483400
C	-3.34503300	-0.45437000	-0.00618100
C	-3.78231600	-1.78489500	-0.02750300
C	-5.13154300	-2.08574000	-0.01848800
C	-6.06477600	-1.04680500	0.01213700
C	-5.65352200	0.27485500	0.03345000
O	-3.94045000	1.88730600	0.04634900
C	-1.93486200	-0.12184600	-0.01521600
N	-1.41975900	1.07298100	0.00234800
C	-0.04439200	0.87920000	-0.01767400
C	0.19536000	-0.47870000	-0.04708300
O	-1.01092200	-1.12151500	-0.04548700
C	1.02575200	1.81354800	-0.01422000
C	2.34906200	1.28282400	-0.03888700
C	2.51066600	-0.13349400	-0.06846700
C	1.47605600	-1.03248500	-0.07052900
O	3.73075500	-0.71808100	-0.10380200
C	2.02728700	-2.42342900	-0.14204500
C	3.44997400	2.16863000	-0.03388700
C	3.24766100	3.52559900	-0.00676300
C	1.93764000	4.05026700	0.01697500
C	0.84900200	3.21402600	0.01375500
C	3.55397400	-2.17385900	0.02798100
C	4.38939200	-2.81994200	-1.06099300
C	4.03376800	-2.54447000	1.42284600
H	-3.04224800	-2.57689900	-0.05126800
H	1.80046900	-2.89843400	-1.10232000
H	1.64412900	-3.07830100	0.64512800
H	4.45195700	1.75487900	-0.05145200
H	4.09645300	4.20099000	-0.00268400
H	1.79211300	5.12521300	0.03830400
H	-0.15893800	3.61422800	0.03254700
H	4.05680300	-2.48742300	-2.04706900

H	4.29277100	-3.90754900	-1.01179100
H	5.44440600	-2.56204700	-0.94129800
H	3.95031900	-3.62345100	1.57689300
H	5.07790000	-2.25299800	1.55791900
H	3.42895600	-2.04059400	2.18139200
H	-6.36862000	1.08941600	0.05723500
H	-7.12596100	-1.27336400	0.01950400
H	-5.45992900	-3.11850900	-0.03502600
H	-2.95505300	1.94890700	0.03681700

Compound 4 - S_0 - DMSO

C	3.98890100	-0.12905700	-0.00883300
C	3.00999100	-1.14050600	-0.02653000
C	3.37445100	-2.49487300	-0.03325700
C	4.70787700	-2.84476000	-0.02372600
C	5.68370700	-1.83899800	-0.00887700
C	5.33755100	-0.50048800	-0.00187800
O	3.66803400	1.16229800	-0.00675600
C	1.65261600	-0.69750000	-0.04559500
N	1.27446800	0.56204800	-0.03430300
C	-0.12832200	0.57081800	-0.05714900
C	-0.51014000	-0.75267200	-0.07699100
O	0.61746100	-1.53867000	-0.07481100
C	-1.09527800	1.61623800	-0.05432500
C	-2.46466300	1.20931100	-0.05131000
C	-2.77162600	-0.18238500	-0.06885100
C	-1.83398900	-1.18076100	-0.08312800
O	-4.04037400	-0.63865500	-0.07842400
C	-2.51946100	-2.51095600	-0.13366700
C	-3.48397400	2.18662800	-0.03427000
C	-3.16580500	3.52037800	-0.02513800
C	-1.81542300	3.92337000	-0.04031300
C	-0.80032500	2.99913300	-0.05581200
B	2.33380200	1.73658600	0.07446900
F	2.13134800	2.61111600	-0.97781400
F	2.14101400	2.37540200	1.28386800
C	-4.01278800	-2.10814700	0.04514100
C	-4.52439700	-2.43335500	1.43930100
C	-4.91228800	-2.65750100	-1.04557600
H	2.59833400	-3.25192400	-0.04645500
H	-2.19510200	-3.18995700	0.65919000
H	-2.34968700	-3.01660400	-1.08964600
H	-4.51684100	1.85798200	-0.02919500
H	-3.95162500	4.26770300	-0.01104600

H	-1.57345300	4.98092000	-0.04393300
H	0.23024000	3.32326400	-0.09133900
H	-5.53277900	-2.03702100	1.57828200
H	-3.86957200	-1.99847200	2.19889700
H	-4.55213500	-3.51594700	1.58711700
H	-4.92662000	-3.74949300	-1.00300800
H	-5.93495900	-2.29405700	-0.92047000
H	-4.54978400	-2.35432200	-2.03052200
H	6.08915300	0.28012200	0.01019800
H	6.73354100	-2.11306600	-0.00184700
H	4.99907900	-3.88835200	-0.02828900

Compound 1 - S_1 - DMSO

C	0.79503700	4.37432700	0.27913700
C	1.50208800	3.12218000	0.13347200
C	2.92617200	3.16940000	0.02580000
C	3.59443400	4.37119700	0.06014000
C	2.88956700	5.57764000	0.20216300
C	1.49971700	5.56779500	0.31014600
C	0.78888600	1.93031500	0.10354300
N	-0.56221400	1.77300400	0.19940200
C	-0.78223400	0.46015300	0.11878700
C	0.45415500	-0.22280100	-0.02937000
O	1.44726500	0.70915200	-0.03773200
C	-1.99984400	-0.29816500	0.16972700
C	-1.87638200	-1.71829500	0.05935700
C	-0.59001700	-2.32849400	-0.08823100
C	0.61357500	-1.58000700	-0.12829300
O	-0.58801100	-3.66624700	-0.16113100
C	0.62565200	-4.38259900	-0.54968000
C	1.95168100	-2.25228900	-0.24293300
C	1.82773300	-3.72701500	0.12735000
C	0.70792500	-4.35311600	-2.07299500
C	0.40430000	-5.79565500	-0.03796400
C	-3.05709800	-2.49117800	0.09877100
C	-4.29111800	-1.88783500	0.24481200
C	-4.40134100	-0.49532800	0.35514400
C	-3.25773300	0.28846300	0.31555300
H	3.46632400	2.23640400	-0.08333000
H	4.67625900	4.38633300	-0.02318800
H	2.67214600	-1.75376600	0.41139400
H	2.33989000	-2.14254500	-1.26182700
H	1.70656800	-3.82806400	1.21069800
H	2.73293800	-4.27208900	-0.15077600
H	0.75556800	-3.33155500	-2.45563800
H	1.59964100	-4.88753000	-2.40991300

H	-0.17035800	-4.83813600	-2.50436100
H	-0.50386000	-6.22030900	-0.47183700
H	0.30825900	-5.80075500	1.05009200
H	1.24937300	-6.42945100	-0.31612700
H	-2.98092500	-3.56799500	0.01178100
H	-5.18493500	-2.50230500	0.27310800
H	-5.37501200	-0.03225300	0.46926000
H	-3.32497600	1.36821100	0.39659300
O	-0.54247400	4.41064200	0.38642700
H	-0.89362600	3.48506600	0.34792000
H	0.93662500	6.48829700	0.42060800
H	3.42401400	6.52114000	0.22821600

Compound 2 - S_1 - DMSO

C	-4.10787700	1.59157600	0.97174700
C	-2.84419900	2.28777400	0.91555200
C	-2.80790500	3.67293400	1.24771900
C	-3.96546700	4.32416000	1.60592900
C	-5.19283300	3.63783600	1.64952100
C	-5.25535400	2.28290700	1.33482700
O	-4.18374400	0.30123500	0.65899100
C	-1.74836300	1.55045400	0.52311700
N	-1.75771200	0.20452800	0.20606300
C	-0.48212400	-0.14307600	-0.09534500
C	0.31282200	1.01622600	0.03875800
O	-0.47610800	2.06269500	0.41170100
C	0.13886600	-1.37605400	-0.46923200
C	1.55653800	-1.34187300	-0.65955200
C	2.29349600	-0.11952000	-0.50072900
C	1.67154000	1.09180100	-0.14030700
O	3.60648300	-0.20444400	-0.69989100
C	4.43104200	1.00748200	-0.77162900
C	2.46139300	2.35031300	0.07226500
C	3.93453300	2.00684400	0.27038400
C	4.33636100	1.53176000	-2.20043700
C	5.83335000	0.52047100	-0.45226500
C	2.21914000	-2.53037000	-1.01826100
C	1.51817000	-3.70748600	-1.18508400
C	0.12863700	-3.73334700	-1.01173300
C	-0.55329700	-2.58236500	-0.66303700
B	-3.06750100	-0.62428100	0.46905100
F	-3.34763400	-1.42008500	-0.63155800
F	-2.88101200	-1.40240400	1.59883700
H	-1.85931900	4.19544400	1.20913400
H	-3.93191700	5.37911200	1.85671500
H	2.07325800	2.88512300	0.94311400
H	2.32983300	3.02256000	-0.78259200

H	4.08194900	1.56985800	1.26302800
H	4.55021800	2.90751600	0.21692100
H	4.95003600	2.42945000	-2.30749400
H	3.30962200	1.78397500	-2.47335200
H	4.70029400	0.77742900	-2.90105700
H	6.13977000	-0.25187400	-1.16121600
H	5.87792700	0.10794400	0.55801400
H	6.53838800	1.35187800	-0.52062700
H	3.29173700	-2.50537400	-1.16365500
H	2.04718500	-4.61341400	-1.45999400
H	-0.41915700	-4.65752800	-1.15835900
H	-1.63004000	-2.59688100	-0.56489700
H	-6.09720200	4.16490800	1.93324600
H	-6.19233900	1.73799400	1.36707400

Compound 3 - S_1 - DMSO

C	1.29900500	4.73730900	0.01021600
C	1.82108200	3.39260800	-0.00997000
C	3.23791400	3.22715800	-0.05037400
C	4.07419300	4.31966700	-0.06927000
C	3.54766400	5.62076100	-0.04925700
C	2.16880200	5.81737200	-0.00984800
O	-0.02231600	4.97394500	0.04810800
C	0.94257900	2.31282700	0.01039600
N	-0.41634900	2.35799800	0.05079600
C	-0.82966000	1.08999800	0.05567800
C	0.30595200	0.22697300	0.01611000
O	1.42218800	1.00497200	-0.00969000
C	-2.16190000	0.54151900	0.09829300
C	-2.28318000	-0.88847100	0.09153900
C	-1.10163600	-1.66140600	0.04814100
C	0.20783600	-1.13112500	0.01018700
O	-1.10530700	-2.99773700	0.03892400
C	1.18541400	-2.26321000	0.01123200
C	-3.57453800	-1.45950900	0.12556300
C	-4.69355500	-0.65129700	0.16783800
C	-4.57052800	0.74487200	0.17629500
C	-3.30992100	1.32995900	0.14067300
C	0.26875800	-3.50281700	-0.16853700
C	0.49674200	-4.57880500	0.87515700
C	0.31204000	-4.04785500	-1.58739900
H	3.63956700	2.22078900	-0.06572500
H	1.73773000	-2.31215800	0.95525300
H	1.91955900	-2.19256400	-0.79518900
H	-3.67285000	-2.53919300	0.11814700
H	-5.67918200	-1.10414500	0.19424900
H	-5.45664900	1.36856600	0.20971900
H	-3.20489100	2.40976000	0.14455000
H	0.39285600	-4.16676200	1.88139500

H	1.50492100	-4.98723800	0.77069000
H	-0.22005800	-5.39372400	0.75166900
H	1.29919700	-4.46805100	-1.79516700
H	-0.43529100	-4.83341800	-1.71833100
H	0.11649200	-3.25236200	-2.31102100
H	1.74204100	6.81447800	0.00607500
H	4.21228000	6.47783400	-0.06446600
H	5.14885800	4.17311800	-0.09994700
H	-0.50325700	4.10870400	0.05909600

Compound 4 - S_1 - DMSO

C	-4.16002600	1.70504300	-0.64089600
C	-2.89028300	2.38616700	-0.68413700
C	-2.86453900	3.77246400	-1.01009300
C	-4.03803900	4.43666000	-1.28301000
C	-5.27065000	3.76090300	-1.24427600
C	-5.32354300	2.40686700	-0.92434200
O	-4.22468200	0.40829300	-0.34944500
C	-1.77051000	1.62841600	-0.41317900
N	-1.76926600	0.28558300	-0.08844300
C	-0.48170400	-0.07595400	0.13509000
C	0.31233200	1.08309400	-0.06311400
O	-0.48838300	2.12655800	-0.41291700
C	0.13249300	-1.31834700	0.51098800
C	1.55483000	-1.30920100	0.70452000
C	2.26446600	-0.10159500	0.48974400
C	1.66590900	1.10600200	0.10118600
O	3.57911700	0.00218200	0.63652000
C	2.72194900	2.15438300	-0.03855800
C	2.20990000	-2.49282800	1.09300700
C	1.49437600	-3.65657500	1.28063500
C	0.10765400	-3.67194600	1.07512000
C	-0.56351800	-2.52304000	0.69342400
B	-3.14522800	-0.44083900	0.14747100
F	-3.16846700	-1.63476900	-0.55877000
F	-3.29277300	-0.67614000	1.50372900
C	4.01349700	1.39874300	0.38193900
C	4.59053700	1.90597100	1.69144500
C	5.04795800	1.32632800	-0.72535000
H	-1.91020100	4.28508100	-1.04012000
H	2.53685000	3.01643900	0.60785900
H	2.79266200	2.52355000	-1.06574300
H	3.28371000	-2.47220800	1.23963300

H	2.00773000	-4.56337800	1.58073700
H	-0.44747100	-4.59347600	1.21026500
H	-1.62767100	-2.55655500	0.50566700
H	5.42911800	1.28230600	2.00822200
H	3.83010200	1.90048600	2.47600100
H	4.94820200	2.93053400	1.56405000
H	5.41282900	2.33057800	-0.95417000
H	5.89645900	0.71087400	-0.41902200
H	4.61225300	0.90153900	-1.63258000
H	-6.26596700	1.87169600	-0.88706800
H	-6.18819400	4.29657900	-1.46200100
H	-4.01209600	5.49234600	-1.53149200

Cell Staining Procedure

In this work, PC-3 cells (prostate cancer cell lines) were used. They were cultivated in an RPMI-1690 medium plus 10% fetal bovine serum and 1% penicillin/streptomycin at 37 ºC in 5% CO_2 atmosphere. These cells were seeded in glass bottom dishes (MatTek Corporation) and allowed to adhere overnight at 37 ºC in 5% CO_2 atmosphere. Confluence was reached after 48 hours of incubation and the medium was replaced by 500 µL fresh one.

Samples (diluted in DMSO), **1**, **2**, **3** and **4** (100 µM), were used directly in cell cultures and incubated for 10 minutes at 37 ºC in a 5% CO_2 atmosphere. As a negative control, the PC-3 cells were incubated under the same conditions with only DMSO at the same dilution used in the staining procedures. The samples were analyzed by using a Carl Zeiss LSM710 Confocal Microscopy. The assays were performed by experimental triplicate in three independent series.

Acridine orange (AO) staining of PC3 prostate cancer cells was performed to counter staining. After 10 minutes incubation at 37°C with the compounds, 1 µL of aqueous AO solution (100 µg/mL of AO in PBS) was added just prior to confocal microscopy acquisition.

To label mitochondria, cells are simply incubated with MitoTracker® Red CMXRos (Molecular Probes), which passively diffuse across the plasma membrane and accumulate in active mitochondria. Before incubation with samples, cells were incubated with 0.5 µM of mitotracker for 20 minutes under growth conditions. Medium replacement was done after incubation time. Afterwards the compounds **1**, **2**, **3** and **4** were incubated with PC3 cells for 10 minutes at 37°C.

Caveolin-1 immunodetection assay

Cells were seeded on 13 mm round glass coverslips on the bottom of a 24-well plate, allowed to adhere overnight and washed three times with serum-free medium for removal of non-adherent cells. After reaching confluence, cells were washed three times with PBS 1X (pH 7.4) and incubated with compounds **2**, **3** or **4** (15 µM as the final concentration from DMSO stock solutions) for 15 minutes at room temperature (DMSO final concentration was down to 0.01% to prevent cell death). The cells were then washed three times with PBS 1X (pH 7.4) at room temperature (RT) and fixed for 30 minutes in

3.7% formaldehyde-PBS solution at RT. The samples were washed three times with PBS 1X (pH 7.4) at RT and permeabilized with detergent buffer (Triton X-100 0.1% in PBS, pH 7.4) for 20 minutes at RT, washed three times with PBS 1X (pH 7.4) at RT and incubated with blocking solution (1% dry milk, 2.5% bovine serum albumin and 8% fetal bovine serum in PBS 1X, pH 7.4) for 20 minutes at RT. The samples were incubated overnight with commercially available rabbit anti-caveolin-1 primary antibody (1:500 dilution) at 4 °C, washed three times with PBS 1X (pH 7.4) at RT and incubated with goat anti-rabbit Alexa-546 secondary antibody for 1 hour at 37 °C in the dark. The cells were again washed three times with PBS 1X (pH 7.4) at RT and incubated with DAPI (300 nM - Invitrogen, Oregon, USA), according to the manufacturer's recommendations. Two negative controls were used: 1) the cells incubated only with DMSO in the same dilution used in the staining procedures; 2) cells incubated only with secondary antibody. The coverslips were mounted using ProLong Gold Antifade (Invitrogen, Oregon, USA) according to the manufacturer's recommendations. Samples were analyzed using a Leica Confocal Microscopy TCS SP5 optimizing to the maxima fluorescent signal irradiating at 405-488 nm.

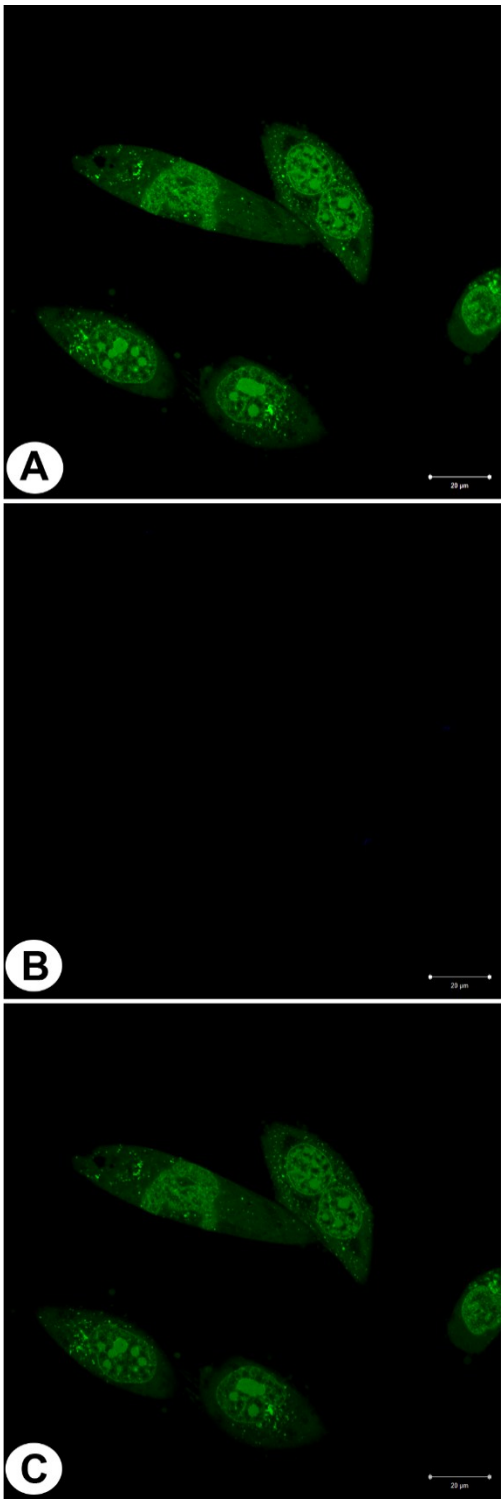

Figure S41. Live PC3 cancer cells stained with **1** (no emission). (A) Positive control with cells stained using the commercially available acridine orange (green emission). (B) **2** as the bioprobe and (C) Overlay of (A) and (B). **1** did not emitted fluoresce at the experimental conditions. Reference scale bar 20 μm.

Pseudo-colour staining pattern using dyes 2-4

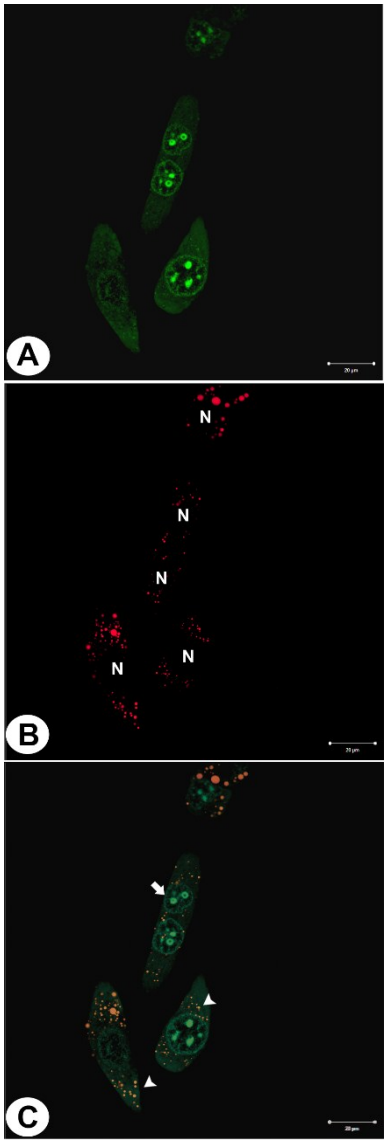

Figure S42. Live PC3 cancer cells stained with **2** (red emission as the pseudo-colour – see the main text for the true colour). (A) Positive control with cells stained with acridine orange (green emission). (B) **2** as the bioprobe and (C) Overlay of (A) and (B). **2** was found accumulated inside of spherical membranous organelles associated with endosomes (white arrow heads). White arrows show the nucleus stained with acridine orange (non-specific staining). N = cell nucleus. Reference scale bar 20 μm.

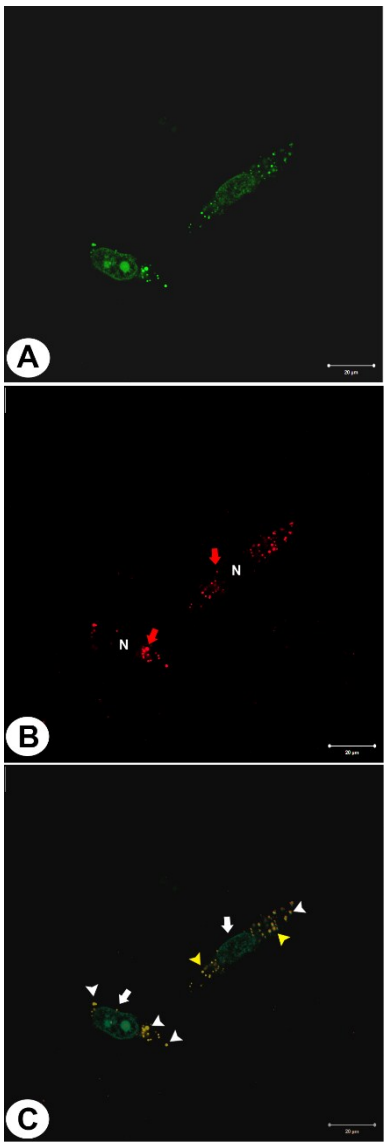

Figure S43. Live PC3 cancer cells stained with **3** (red emission as the pseudo-colour – see the main text for the true colour). (A) Positive control with cells stained with acridine orange (green emission). (B) **3** as the bioprobe and (C) Overlay of (A) and (B). **3** was found accumulated inside of spherical membranous organelle correlated with early endosomes (white arrow heads), late endosomes (yellow arrow heads) and lysosomes (red arrows). White arrows show the nucleus stained with acridine orange (non-specific staining). N = cell nucleus. Reference scale bar 20μm.

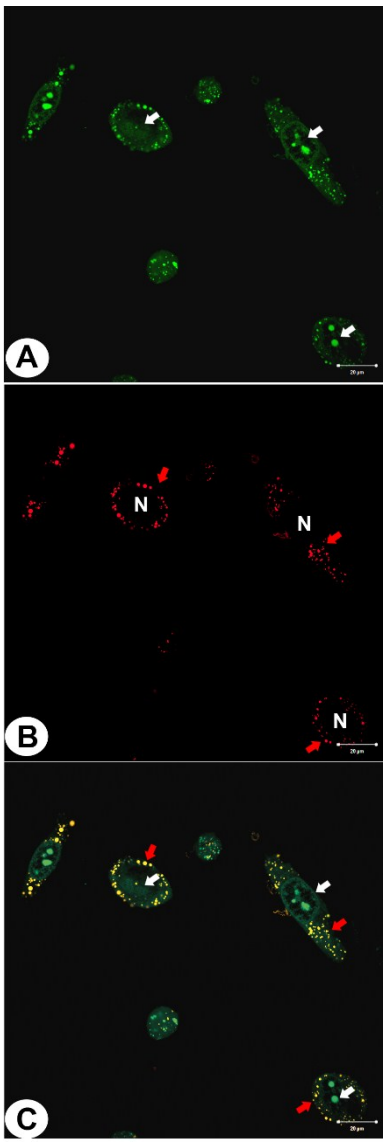

Figure S44. Live PC3 cancer cells stained with **4** (red emission as the pseudo-colour – see the main text for the true colour). (A) Positive control with cells stained with acridine orange (green emission). (B) **4** as the bioprobe and (C) Overlay of (A) and (B). **4** was localized inside of spherical membranous organelles belong to the endocytic pathway. Red arrows show the staining membranous compartment correlated with lysosomes. White arrows show the nucleus stained with acridine orange (non-specific staining). N = cell nucleus. Reference scale bar 20 μm.

Cytotoxicity against cancer cell lines – MTT assay

The cytotoxic activity of the compounds were evaluated by MTT assay,[25] against PC3 (human prostate cancer cell line) obtained from the National Cancer Institute (Bethesda, MD, USA). The cell was maintained in an RPMI 1640 medium supplemented with 10% fetal bovine serum, 2 mM glutamine, 100 U/mL penicillin and 100 μg/mL streptomycin, at 37 °C with 5% CO_2. Cancer cell growth was quantified by the ability of living cells to reduce the yellow dye 3-(4,5-dimethyl-2-thiazolyl)-2,5-diphenyl-2H-tetrazolium bromide (MTT) to a purple formazan product. Briefly, cells were plated in 96-well plates (0.1 x 10^6 cells/mL) and compounds, dissolved in DMSO, were added to each plate well in a final concentration of 200 μM. Control groups received the same amount of vehicle. After 60 minutes of incubation, the supernatant was replaced by fresh medium containing MTT (0.5 mg/mL). Three hours later, the MTT formazan product was dissolved in 150 μL DMSO and absorbance was measured at 595 nm (DTX-880, Beckman Coulter®). The final concentration of DMSO in the culture medium was kept constant, below 0.1% (v/v). All cell treatments were carried out with three replicates.

Electrochemical studies

Cyclic voltammetry (CV) experiments were performed with a conventional three electrode cell in an Autolab PGSTAT-30 potentiostat (Echo Chemie, Utrecht, the Netherlands) coupled to a microcomputer, using GPES 4.9 software. The working electrode was a glassy carbon (GC) BAS (d = 3 mm), the counter electrode was a Pt wire and the reference electrode an Ag|AgCl, Cl^- (sat.), all contained in a one-compartment electrochemical cell with a volumetric capacity of 10 mL. The GC electrode was cleaned up by polishing with alumina on a polishing felt (BAS polishing kit). Extra dry 99.8% *N,N*-Dimethylformamide (Acros Organics) was used as solvent. In CV experiments, the scan rate varied from 10 to 500 mV s^{-1}. Electrochemical reduction was performed in aprotic media (DMF + $TBAPF_6$ 0.1 mol L^{-1}), at room temperature (25 ± 2 °C). Each compound (**1**-**4**) (1 x 10^{-3} mol L^{-1}) was added to the supporting electrolyte and the solution was deoxygenated with argon before the measurements by cyclic voltammetry. Different potential ranges were used, from cathodic to anodic scan. The most representative one was from 0 to -3.0 V *vs*. Ag|AgCl, Cl^- (sat.) and it was chosen for the investigation and

representation of all of the compounds. Anodic scans until +1.0 V were performed and no well-developed anodic wave was evidenced.

Results and Discussion

Aryl-substituted oxazoles and their boron complexes were subjected to several electrochemical studies. Earlier, on mercury electrodes, in aprotic media, the oxadiazoles and 2-naphthyl-substituted oxazoles were shown to be reduced via a two-electron ECE process at large concentration of proton donors in relation to the analyzed compounds,[26,27] while on carbon fibers, in DMF + $TBAPF_6$ 0.1 mol L^{-1}, two monoelectronic waves are evidenced, the first one with a quasi-reversible nature and the second irreversible,[28] due to a fast chemical protonation reaction, with the supporting electrolyte as a proton source. In all cases, those heterocycles were shown to be reducible at rather negative potentials (*E*pc > -2.0 V vs Ag|AgCl). In the present case, in DMF, the cyclic voltammograms of all the analyzed compounds (**1**-**4**) displayed two reduction waves. The first electron uptake results in relatively stable radical anions, for the uncomplexed compounds or radicals, in the boron-complexed ones, while the second reduction processes presumably result in dianions, followed by protonation, forming dihydro derivatives for **1** and **3**. On the other, for compounds **2** and **4**, the additional electron capture can lead to the cleavage of the N-B bonding, giving back the original oxazole, as shown by the presence of a reduction wave in the reverse scan. Differences in current are noticed among the phenolic derivatives, when compared to the respective boron complexes. As shown in Figure S45, the comparison of the electrochemical behaviors of the four compounds allows us to suggest that the complexation with boron difluoride (**2** and **4**) slightly facilitates the reduction process (Table S10), since less negative Epc values are obtained in comparison with the ones obtained for the free compounds (**1** and **3**). The reduction of the iminium cation is easy, compared to the precursor imine. Compound **4** was chosen for a more complete electrochemical investigation. Its cyclic voltammograms shows two main reduction processes and a third one, very close to the supporting electrolyte discharge. A first reduction peak with a corresponding re-oxidation peak in the back scan is found at -2.059 V and -1.950 V vs. Ag|AgCl|Cl^- (sat.) respectively. The difference in peak potentials is large (ΔEp = 109 mV). At this potential a one-electron transfer takes place. A second reduction peak is observed at -2.574 V vs. Ag|AgCl|Cl- (sat.) and no re-oxidation peak is noticed. This is characteristic of an irreversible system, which is

possibly related to the dissociation of the complex. Upon potential inversion at -2,652 V, a reduction wave (see arrow) is observed in the anodic counterpart of the CV. This cleavage would lead to an addition reduction wave (Epc3). Additional studies for a complete understanding of the reduction process are underway.

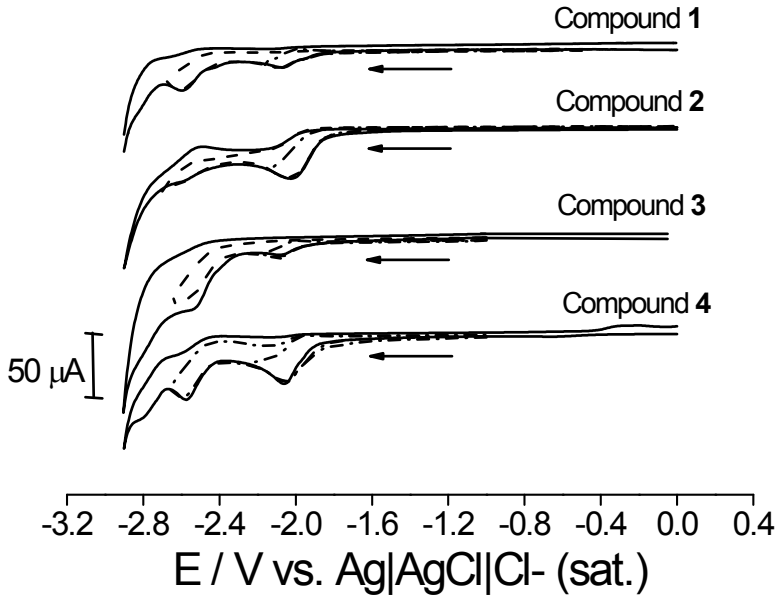

Figure S45. Cyclic voltammograms of compounds **1**, **2**, **3** and **4**, c = 1 x 10^{-3} mol L^{-1}, DMF/$TBAPF_6$, 0.1 mol L^{-1}, ν = 100 mV s^{-1}. Cathodic direction. Glassy carbon electrode.

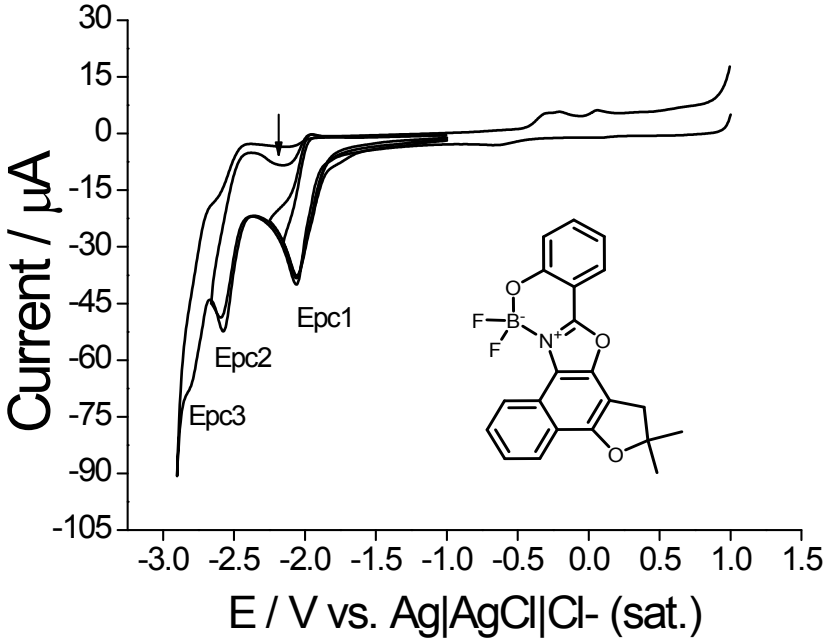

Figure S46. Cyclic voltammograms of compound **4**, c = 1 x 10^{-3} mol L^{-1}, DMF/$TBAPF_6$, 0.1 mol L^{-1}, ν = 100 mV s^{-1}. Cathodic direction. Glassy carbon electrode.

Table S10. Major electrochemical parameters of the substituted 2-phenyl-1,3-oxazoles (c = 1 x 10^{-3} mol L^{-1}), in DMF/$TBAPF_6$, 0.1 mol L^{-1}, ν = 100 mV s^{-1}.

Compounds	Epc_1 (V)	E_{redox} (V)	Epc_2 (V)	Epa_1 (V)
1	-2.069	-2.038	-2.604	-1.250
2	-2.035	-1.943	-2.616	-1.961
3	-2.079	-2.031	-2.530	-1.983
4	-2.059	-2.010	-2.574	-1.951

References

1. S. L. de Castro, F. S. Emery and E. N. da Silva Júnior, *Eur. J. Med. Chem.*, 2013, **69**, 678.

2. K. C. G. de Moura, K. Salomão, R. F. S. Menna-Barreto, F. S. Emery, M. C. F. R. Pinto, A. V. Pinto and S. L. de Castro, *Eur. J. Med. Chem.*, 2004, **39**, 639.

3. K. C. G. de Moura, F. S. Emery, C. N. Pinto, M. C. F. R. Pinto, A. P. Dantas, K. Salomão, S. L. de Castro and A. V. Pinto, *J. Braz. Chem. Soc.*, 2001, **12**, 325.

4. A. V. Pinto, C. Neves Pinto, M. C. F. R. Pinto, R. M. Santa Rita, C. Pezzella and S. L. de Castro, *Arzneim-Forsch.*, 1997, **47**, 74.

5. C. Neves-Pinto, A. P. Dantas, K. C. G. Moura, F. S. Emery, P. F. Polequevitch, M. C. F. R. Pinto, S. L. de Castro and A. V. Pinto, *Arzneim-Forsch.*, 2000, **50**, 1120

6. L. F. Fieser and M. Fieser, *J. Am. Chem. Soc.*, 1948, **70**, 3215.

7. J. W. Lyga, R. N. Henrie, G. A. Meier, R. W. Creekmore, and R. M. Patera, *Magn. Res. Chem.*, 1993, **31**, 323-328.

8. I. D. Rae, J. A. Weigold, R. H. Contreras, and R. R. Biekofsky, *Magn. Res. Chem.*, 1993, **31**, 836-840.

9. R. A. Cormanich, M. A. Moreira, M. P. Freitas, T. C. Ramalho, C. P. Anconi, R. Rittner, R. H. Contreras, C. F. Tormena, *Magn. Res. Chem.*, 2011, **49**, 763-767.

10. Enraf-Nonius COLLECT; B. V. Nonius: Delft, The Netherlands, (1997-2000).

11. Z. Otwinowski and W. Minor, in: C.W. Carter and R.M. Sweet (Eds.), Methods in Enzymology, vol. 276, Academic Press, New York, (1997), p. 307-326.

12. CRYSALISPRO, Agilent Technologies, Version 1.171.35.21 (release 20-01-2012 CrysAlis171.NET.

13. SCALE3 ABSPACK scaling algorithm. CrysAlis, Agilent Technologies, Version 1.171.35.21 (release 20–01-2012 CrysAlis171.NET).

14. G. M. Sheldrick, SHELXS-97. Program for Crystal Structure Resolution. University of Göttingen, Göttingen, Germany, (1997).

15. G. M. Sheldrick, SHELXL-97. Program for Crystal Structure Refinement. University of Göttingen, Göttingen, Germany, (1997).

16. L. J. Farrugia, *J. Appl. Cryst.* 1997, **30**, 565-566.

17. L. J. Farrugia, *J. Appl. Cryst.* 1999, **32**, 837-838.

18. A. T. R. Williams, S. A. Winfield and J. N. Miller, *Analyst* 1983, **108**, 1067-1071.

19. W. H. J. Melhuish, *Phys. Chem.* 1961, **65**, 229-235.

20. T. Owen, Fundamentals of modern UV-visible spectroscopy. (2000) Agilent Technologies.

21. M. J. Frisch, G. W. Trucks, H. B. Schlegel, G. E. Scuseria, M. A. Robb, J. R. Cheeseman, G. Scalmani, V. Barone, B. Mennucci, G. A. Petersson, H. Nakatsuji, M. Caricato, X. Li, H. P. Hratchian, A. F. Izmaylov, J. Bloino, G. Zheng, J. L.

Sonnenberg, M. Hada, M. Ehara, K. Toyota, R. Fukuda, J. Hasegawa, M. Ishida, T. Nakajima, Y. Honda, O. Kitao, H. Nakai, T. Vreven, J. A. Montgomery, J. E. Peralta, F. Ogliaro, M. Bearpark, J. J. Heyd, E. Brothers, K. N. Kudin, V. N. Staroverov, R. Kobayashi, J. Normand, K. Raghavachari, A. Rendell, J. C. Burant, S. S. Iyengar, J. Tomasi, M. Cossi, N. Rega, J. M. Millam, M. Klene, J. E. Knox, J. B. Cross, V. Bakken, C. Adamo, J. Jaramillo, R. Gomperts, R. E. Stratmann, O. Yazyev, A. J. Austin, R. Cammi, C. Pomelli, J. W. Ochterski, R. L. Martin, K. Morokuma, V. G. Zakrzewski, G. A. Voth, P. Salvador, J. J. Dannenberg, S. Dapprich, A. D. Daniels, J. B. Farkas, J. B. Foresman, J. V. Ortiz, J. Cioslowski, and D. J. Fox, (2009) Gaussian 09, Revision A.02, Wallingford CT.

22. T. Yanai, D. Tew, and N. Handy, *Chem. Phys. Lett.* 2004, **393**, 51-57.

23. T. L. Fonseca, H. C. B. de Oliveira, M. A. and Castro, *Chem. Phys. Lett.* 2008, **457**, 119-123.

24 (a) S. Miertus, E. Scrocco, and J. Tomasi, *Chem. Phys.* 1981, **55**, 117-129. (b) R. Cammi, and J. Tomasi, *J. Comput. Chem.* 1995, **16**, 1449-1458. (c) J. Tomasi, B. Mennucci, and R. Cammi, *Chem. Rev.* 2005, **105**, 2999-3093.

25. T. J. Mosmann, *Immunol. Methods*, 1983, **65**, 55-63.

26. G. L. Smith, L. D. Cook and J. W. Rogers, *J. Electrochem. Soc.* 1972, **119**, 1332-1338.

27. L. Henning and H. Ole. Organic Electrochemistry. Fourth Edition, Marcel Dekker, Inc, New York (2001) pp. 692.

28. L. Kress, A. Neudeck, A. Petr and L. Dunsch, *J. Electrochem. Soc.* 1996, **414**, 31-40.